FEDERAL UNIVERSITY OF ITAJUBÁ - UNIFEI
GRADUATE PROGRAM IN
ELECTRICAL ENGINEERING

The Use of Advanced Signal Processing and Deep Learning for Pattern Recognition in Integrated Metrics of Quality Performance: A Smart Grid Application

Rafael de Souza Salles

Itajubá, December 04, 2020

FEDERAL UNIVERSITY OF ITAJUBÁ - UNIFEI
GRADUATE PROGRAM IN
ELECTRICAL ENGINEERING

Rafael de Souza Salles

The Use of Advanced Signal Processing and Deep Learning for Pattern Recognition in Integrated Metrics of Quality Performance: A Smart Grid Application

Dissertation submitted to the Graduate Program in Electrical Engineering as part of the requirements to obtain the title of **Master of Science in Electrical Engineering.**

Concentration Area: Electrical Power Systems

Supervisor: Prof. Dr. Benedito Isaías Lima Fuly
Co-supervisor: Prof. Dr. Paulo Fernando Ribeiro

December 04, 2020
Itajubá

Rafael de Souza Salles

The Use of Advanced Signal Processing and Deep Learning for Pattern Recognition in Integrated Metrics of Quality Performance: A Smart Grid Application

Dissertation submitted to the Graduate Program in Electrical Engineering as part of the requirements to obtain the title of **Master of Science in Electrical Engineering.**

Work approved. Itajubá, December 4, 2020:

_____
Prof. Dr. Benedito Isaías Lima Fuly
Federal University of Itajubá (Supervisor)

_____
Prof. Dr. Paulo Fernando Ribeiro
Federal University of Itajubá (Co Supervisor)

_____
Prof. Dr. Cairo Lúcio Nascimento Júnior
Aeronautical Technological Institute, Brazil

_____
Prof. Dr. Carlos Augusto Duque
Federal University of Juiz de Fora, Brazil

_____
Prof. Dr. Giscard Francimeire Cintra Veloso
Federal University of Itajubá, Brazil

_____
Prof. Dr. Guilherme Sousa Bastos
Federal University of Itajubá, Brazil

Itajubá, December 04, 2020

Acknowledgements

I want to thank Professor Benedito Isaías Lima Fuly for having welcomed me with open arms since the first moment at UNIFEI and supporting my development as a master's student and my research. Thanks also for the trust you have placed in me.

I would also like to express my deeply thanks to Professor Paulo Fernando Ribeiro for the guidance provided, for the encouragement and confidence in my work. I also want to emphasize that all the opportunities and knowledge delegated to me were crucial to becoming a better professional and human being. I really appreciate all the support and dedication to my research.

I would like to thank my fellow researchers, professors and also some members of aPTIs-SG^2 group who in addition to developing works together, also provided support and moments of joy. It is through networks that we will achieve quality research and development.

Finally, I would like to thank my family and closest friends Márcia, Patrícia, Selma, Roberto, and Roberta, for their unconditional support for my decisions and dreams.

"If you can fail well, you can do engineering well."
(Ethan Brue)

Resumo

Qualidade de Energia não é uma temática nova, porém de forma alguma deve ser negligenciada, pois seus parâmetros de performance indicam problemas na adequação entre o equipamento do consumidor e a rede elétrica. Com as transformações em andamento nos sistemas elétricos de potência, caracterizados pela alta penetração de fontes renováveis de energia, inserção massiva de componentes baseados em eletrônica de potência na rede e descentralização da geração, essas questões se tornam cada vez mais importantes. Nas Redes Inteligentes, busca-se soluções cada vez mais avançadas para solucionar questões dos distúrbios da Qualidade de Energia. Dentro desse contexto, o processamento avançado de sinais possui um papel importante para tratar as medições da rede e apoiar diversas aplicações. A Inteligência Artificial, tem ganhado grande destaque dar suporte para aplicações com soluções inovadoras em diversas áreas. Esta pesquisa tem como objetivo investigar o uso de processamento avançado de sinais e técnicas de Aprendizagem Profundo ("*Deep Learning*") para reconhecimento de padrões e classificação de sinais com distúrbios da Qualidade de Energia. Para este propósito, a Transformada Wavelet Contínua com um banco de filtros é usada para gerar imagens 2-D no domínio do tempo-frequência a partir de sinais com distúrbios de tensão. O trabalho visa utilizar Redes Neurais Convolucionais para classificar essas imagens de acordo com a respectiva distorção. Nesta implementação de Inteligência Artificial, etapas específicas de projeto, treinamento, validação e teste serão realizadas para um modelo elaborado pelo autor e também utilizando a técnica de transferência de conhecimento com as redes pré-treinadas SqueezeNet, GoogleNet, e ResNet-50. O trabalho foi desenvolvido no software MATLAB/Simulink, todas as etapas de processamento do sinal, projeto de modelos de classificação, simulação e geração dos dados investigados. Todas as etapas tiveram seus objetivos específicos cumpridos, culminando na boa execução e desenvolvimento da pesquisa. Os resultados obtidos mostraram alta precisão para "CNN de Scratch" e ResNet-50 em classificar o conjunto de testes. Os outros dois modelos obtiveram acurácias não tão altas, e os resultados se mostram consistentes ao comparar com outras metodologias. Considerações sobre os resultados foram apontadas. Por fim, algumas conclusões foram estabelecidas, assim como uma reflexão filosófica sobre o papel dos tópicos abordados para os sistemas elétricos de potência.

Palavras-chaves: Qualidade de Energia. Processamento Avançado de Sinais. Inteligência Artificial. Aprendizado Profundo. Redes Neurais Concolucionais. Redes Inteligentes.

Abstract

Power quality (PQ) is not a new theme, but it should not be neglected in any way, as its performance parameters will reveal problems in the adequacy between the consumer equipment and the electrical grid. With the ongoing transformations in electrical power systems, characterized by the high penetration of renewable energy sources, the massive insertion of components based on power electronics in the network, and the decentralization of generation, these issues are becoming increasingly important. In Smart Grids, solutions are sought for more advanced solutions to solve PQ disturbances problems. Advanced signal processing plays an essential role in dealing with the network and supporting various applications within this context and Artificial Intelligence (AI), which has gained significant prominence to feed applications with innovative solutions in several areas. This research investigates the use of advanced signal processing and Deep Learning techniques for pattern recognition and classification of signals with PQ disorders. For this purpose, the Continuous Wavelet Transform with a filter bank is used to generate 2-D images with the time-frequency representation from signals with voltage disturbances. The work aims to use Convolutional Neural Networks (CNN) to classify this data according to the images' distortion. In this implementation of AI, specific stages of design, training, validation, and testing were carried out for a model elaborated by the case file and a knowledge transfer technique with the pre-trained networks SqueezeNet, GoogleNet, and ResNet-50. The work was developed in the MATLAB/Simulink software, all signal processing stages, CNN design, simulation, and the investigated data generation. All steps have their objectives fulfilled, culminating in the excellent execution and development of the research. The results sought high precision for CNN de Scratch and ResNet-50 in classify the test set. The other two models obtained not-so-high accuracy, and the results are consistent when compared with different methodologies. Considerations about the results were pointed out. Finally, some conclusions were established and a philosophical reflection on the role of AI and advanced signal processing in electrical power systems.

Key-words: Power Quality. Advanced Signal Processing. Deep Learning. Convolutional Neural Networks. Smart Grids.

Contents

List of Figures

List of Tables

List of abbreviations and acronyms

AI	Artificial Intelligence
ANN	Artificial Neural Network
CNN	Convolutional Neural Network
CWT	Continuous Wavelet Transform
DAG	Directed Acyclic Graph
DC	Direct Current
DL	Deep Learning
DWT	Discrete Wavelet Transform
FFT	Fast Fourier Transform
HV	High Voltage
ICT	Information and Communication Technology
LSTM	Long Short-Term Memory
LV	Low Voltage
MFCNN	Multifusion Convolutional Neural Network
ML	Machine Learning
MTCNN	Multi-Task Convolutional Neural Network
PQ	Power Quality
PV	Photovoltaic
SG	Smart Grid
SGD	Stochastic Gradient Descent
SNR	Signal to Noise Ratio
SPM	Space Phasor Model
STFT	Short-Time Fourier Transform
SVM	Support Vector Machine
WPT	Wavelet Packet Transform
WVD	Wigner-Ville Distribution

1 Introduction

1.1 General

In the last decades, Power Quality (PQ) has become a significant concern to the power sector due to deregulation, the widespread use of sensitive loads, power electronic devices, and the industrial processes transformation (BOLLEN; GU, 2006). The quality performance problems become more unpredictable due mainly to the increase in distributed generation, wide insertion of renewable energy sources (RES) and electronic-based grid components.

These new challenges are associated with the context of the Smart Grid (SG) development, which has been placed in the focus to seek a more secure, reliable, efficient and robust energy supply. Future distribution systems will based on the simultaneous presence of various distributed resources, such as Photovoltaic (PV) power plants and wind farms, energy storage systems, and controllable/non-controllable loads (BRACALE et al., 2015). It is also characterized by extensive computerization, the key use of large-scale Information and Communication Technology (ICT), automation, and two-way flow of massive data and power. Together, these aspects corroborate a change in the PQ the panorama and a need for a new treatment of these integrated metrics.

PQ is directly associated with the quality of the voltage/current signal fundamental waveform at the analysis point (ARRILLAGA; BOLLEN; WATSON, 2000). The investigation of events that generate deformations in these signals is the main focus of quality analysis. The identification and classification these quality problems is an application of great importance in this field of power systems. With the increase in the grid's complexity, the use of more accurate tools becomes necessary, given the various possibilities of occurrence. The most common disturbances are voltage sag/swell, oscillatory and impulsive transients, harmonics, and flicker. With the recent transformations, the know ones can show new behaviours, and the emerging disturbances gain attention. These events are often associated.

The signal processing has a crucial role in power systems that determine parameters for measurement, the accuracy, and method to provide the best characterization and analysis of the signals to be investigated (RIBEIRO et al., 2013). These parameters (voltage, current, frequency, power, etc) go through several treatment steps from the transducers to the final applications, and this constitutes conduction, conversion, filters, and analysis in different domains. Through advanced processing, it is possible to use techniques to extract patterns and characteristics from the signals. Signals with PQ disturbances are

essentially variations in the fundamental frequency of 50/60 Hz, so multi-domain analyzes are very useful to characterize them.

The pattern recognition uses signal processing techniques in conjunction with classification algorithms, so it is possible to create a cause and effect relationship in the analysis of the signals. This pattern recognition will be important in future power systems due to the variability of electrical signals from diverse generators and loads to help the system operate correctly, identify problems, and control the grid's power delivery process (RIBEIRO et al., 2013). The use of Artificial Intelligence (AI) techniques to assist in the classification process is increasingly recurrent. Although there are several methods, AI is highlighted for emulating the way that the human identifies and recognizes patterns.

In power systems, one of the highly bracing and practicable recent advances is the increasing use of AI techniques at the cutting-edge level of technologies to deal with the complex problems and a new context of massive data/information for power delivery associated with SG (MISHRA et al., 2020). This emphasis given to AI is due to the different systems that are evolving and becoming increasingly complex, demanding sophisticated and computer-based solutions. In this way, SG's phenomenon becomes ideal to flourish ideas and applications that combine advanced fields and innovative techniques.

1.2   Research Objective

This dissertation investigates the use of advanced signal processing and Deep Learning (DL) in pattern recognition applied to signals with PQ disturbances. For this purpose, the Continuous Wavelet Transform (CWT) with a filter bank is used to generate 2-D images in the time-frequency domain from oscillographs with voltage disturbances. This research aims to use Convolutional Neural Network (CNN) to classify these data according to their respective distortion from the images. In this AI implementation, specific design, training, validation, and testing steps will be carried out. This work was developed in the MATLAB/Simulink software, the stages of signal processing, design CNNs, simulation, and the investigated data generation. Below are some specific goals:

1. Highlight the role of advanced signal processing and AI in power systems, especially in this context of SG;

2. Review the state-of-art to verify the importance of the research associated with pattern recognition for integrated metrics of quality performance;

3. Carry out a theoretical foundation to guide the development of the work;

4. Use a CWT-based method to generate scalograms from signals with PQ disturbance to characterize them from a color map;

5. Using Simulink to model a system adapted from IEEE benchmark five bars system;

6. Develop, train, validate, and test CNNs to classify the images generated in the two previous objectives' set within the investigated disorders;

7. Perform a performance analysis of the results obtained;

8. Make data, codes, and methods available in public databases to share with the community of professionals and researchers.

1.3   Research Relevance

Classification of PQ events using pattern recognition is a important field of investigation on electrical power delivery. Combining advanced signal processing methods with AI has proved to be advantageous to meet the electrical sector's needs and developments, mainly in SGs. When using images to extract characteristics from the signals and demonstrating an effective and viable way of visualizing PQ disturbances, it also goes in line with the agenda that has been the development of image-based techniques for pattern recognition in several applications in the world. Finally, DL techniques has gained some attention for applications in power systems., which has been recurring in recent times (MISHRA et al., 2020).

In addition to being innovative, another noteworthy point is that these methods have been widely explored for applications in different fields of knowledge, which is no different for electrical engineering and power systems. The use of CWT scalograms with DL together presents several examples such as detecting respiratory and heart diseases, diagnosing faults in aviation engines, and diagnosing acoustic fractures in structures, among many others (GOU et al., 2020; SHUVO et al., 2020; XIN et al., 2020). Therefore, following this trend of opportunities, the research focused on these methods in applying diagnostics in electrical systems is crucial and innovative.

1.4   Methodology

The method used is based on the first moment in a literature review to substantiate through the raised theoretical background and the previous important work. The procedures of signal processing, modeling, and datasets generation are performed in MATLAB/Simulink and the development stages of DL techniques. The software is very friendly with this type of application, with specific toolboxes for applications of DL, Wavelets, and modeling of power systems.

The final objects of investigation, the CNNs, are elaborated and chosen with two design methods: design from scratch and transfer learning. The methodology also provides

a detailed description of the steps and also the provision of the data used. Qualitative and quantitative analyzes are carried out to highlight the results obtained and the implications. Figure 1.1 illustrates the research scope on the PQ events classification steps.
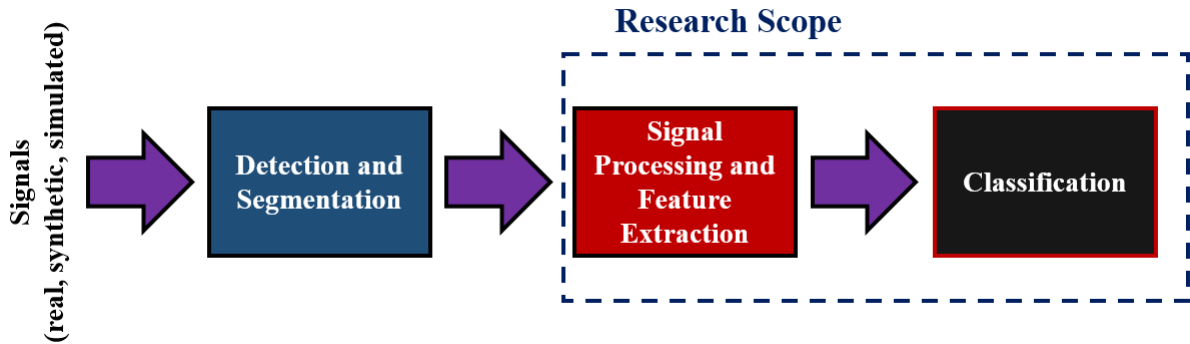
Figure 1.1 – Research scope on the PQ events classification steps.

1.5   Results and Contributions

The results are expected to provide an overview and possibilities of using CNNs to classify images that describe voltage disturbances. In addition to presenting a performance analysis, these results can serve as a reference for choosing and developing projects in the area.

The research brings several contributions since there is not much work in this specific field of application and addresses them together. Then, the work contributes to exemplifying how to design a CNN from scratch and employ transfer learning for image classification in PQ. The use of CWT scalograms to characterize PQ signals also opens the possibility for applications that use 2-D images to classify these issues.It also provides a material of reference for future work. Finally, there is a contribution to bringing a research with an application proposal with cutting edge methods with details to guarantee the findings' reproducibility.

1.6   Dissertation Layout

This dissertation is divided as follows:

Chapter 2 presents a literature review on pattern recognition for PQ disturbances. Besides, the theoretical tools used in this work with advanced signal processing and DL frameworks are presented. Also, the chapter describes an integrated perspective of SG.

Chapter 3 is directed towards the research's development procedures, going through the data generation, featuring extraction, and CNNs design and training steps.

Chapter 4 presents the results obtained in the CNN test stage and also some key considerations.

Finally, chapter 5 brings the work's conclusions, opportunities for future work, and considerations from a philosophical perspective on the research's main theme.

2 Theoretical Background

This chapter presents the theoretical topics necessary for a good understanding of the development of this work. Starting with the state-of-art and going through the other subjects involved in this research.

2.1 State-of-Art

Several works in the literature use pattern recognition to improve power quality events classification. In Cerqueira et al. (2008), a novel Support Vector Machine (SVM) based method for power quality event classification is proposed, and a simple approach for feature extraction is introduced, based on the subtraction of the fundamental component from the acquired voltage signal. The resulting signal is presented to a support vector machine for classification, showing improved performance. Silva, Duque e Ribeiro (2016) introduces the concept and the initial steps for using this powerful tool, here named iPQ-Google, and which can help utilities, customers, and researchers to investigate and easily find, compare and diagnose possible PQ waveform deviations saved on the internet.

In Bhavani e Prabha (2017), the authors introduces a novel automatic hybrid classifier to detect and classify events like Normal, Sag, Swell, and Interruptions are obtained by modeling a three-phase distribution system using MATLAB Simulink. For classification, the system uses the Wavelet Packet Transform (WPT) and Artificial Neural Network (ANN). The classification performance is compared with Fast Fourier Transform (FFT) based ANN. The simulation results obtained have significant improvement over existing methods. The work elaborated by Mahela, Sharma e Manglani (2018) is focused on presenting an approach based on Discrete Wavelet Transform (DWT) and Fuzzy c-means clustering for the detection and classification of PQ events. The disturbances such as voltage sag, voltage swell, momentary interruption, oscillatory transient, impulsive transient, harmonics, notch, and spike are simulated in MATLAB with the help of mathematical expressions. Already in Alshahrani et al. (2015), a detection method and classification technique of power quality disturbances are presented. The wavelet filters detect and extract the features of a disturbance at different frequencies, and the classification is done using artificial neural networks ANN. In Nagata et al. (2020), the authors proposes an innovative approach to detect, segment and classify voltage sags according to their causes. To detect and segment, Independent Component Analysis is used, with the advantage of have a fast execution and with low computational effort in the operational stage. To classify, Higher-Order Statistics are used for feature extraction and the classifiers are based on Neural Networks and SVM. Great results were achieved for the simulated and real

signals.

Focused on DL and signal processing techniques specifically, some works are more linked to the AI methods.The work in Balouji e Salor (2017) in contrast with the existing PQ event data analysis techniques, sampled voltage data of the PQ events are not used, but image files of the three-phase event data are analyzed by taking advantage of the success of the deep leaning approach on image-file-classification. DIGITS DL platform of NVIDIA is employed for the application algorithm on PQ event data images, it is shown that the test data can be classified with 100% accuracy.

The methodology proposed by Wang e Chen (2019) is a classification structure based on CNN considering 1-D signals. At the proposal of a deep CNN, several units are stacked to extract resources from samples of massive disturbances automatically. A typical simulation system is built to analyze the causes of power quality micro-network problems, and field data from a multiple-micro system are used to prove the validity of the proposed method. The work by Gong e Ruan (2020), one dimension's signals are also considered, using an Inception (Resnet) model modified for classification. It proposes two training methods and makes comparisons and classifications with varieties of signals. The technique was impressive from the point of view of accuracy when compared to other methods. In Qiu et al. (2020a) the one-dimensional composite convolution is proposed to improve the diversity of network features based on the standard convolution and dilated convolution. They conduct various experiments to verify the effectiveness of the Multifusion Convolutional Neural Network (MFCNN). Compared with the handcrafted feature design methods and the general CNN models, the simulation under different noises and hardware platform-based experiments verify the performance parameters. The exciting thing about the work in (LI et al., 2020) is that it uses a method that combines empirical mode decomposition (EMD) with 1D-CNN for PQ DC issues. The proposed network was also compared with other state-of-the-art deep neural networks, and the experiment proved its effectiveness. Finally, an example analysis is carried out with the real data to show the validity of the proposed method for evaluating DC issues in a real case. In Wang, Xu e Che (2019), Aggarwal et al. (2019) is also possible to find methodologies that explore alternatives and improvements for DL models for 1-D data classification.

In Dong et al. (2019) was proposed a Multi-Task Convolutional Neural Network (MTCNN) to realize the multi-label classification of multiple power quality disturbances. The experiments have demonstrated that this method had better performance and it can greatly improve the accuracy rate for identifying PQ disturbances under different conditions. In (QIU et al., 2020b), it is proposed a novel detection framework for complex PQ disturbances based on Multifusion Convolutional Neural Network (MFCNN). When compared with the handcrafted feature design methods and the general convolutional neural network models, the simulation under different noises and hardware platform-based

experiments verify the effectiveness of noise immunity, higher training speed, and better accuracy of the method. Lastly, the proposal in Cai et al. (2019) is a hybrid approach combiningWigner-Ville Distribution (WVD) with CNN for PQ disturbance classification. The WVD is used to transform the 1-D signal to 2-D image, and uses the CNN for image classification. This approach is very similar to the one developed in this work, but the feature extraction for 2-D image is different. The high classification accuracy of test results is achieved to confirm the effectiveness of the proposed method. The work Xue et al. (2020) proposed a novel DL method based on deep CNN and spectrogram for PQ disturbances classification is proposed. Considering the characteristics of PQs problems, the spectrogram is used to restructure waveforms, and the convolutional base is designed to capture features, speed up training, and reduce overfitting. Also a novel tagging method for the issues is proposed and the small sample training is realized.

The doctoral thesis Bagheri (2018), conducted at Sweden, proposes particularly a Space Phasor Model (SPM) of the three phase-to-neutral voltages as basis for analytic methods. The SPM is especially suitable as it is a time-domain transform without loss of any information. Another important contribution of the work is that most of the developed methods have been applied to a large dataset of about 6000 real-world voltage dips. Two DL-based (2D-CNN) voltage dip classifier has been developed. In Ekici et al. (2020), a approach for classifying PQ disturbances such as voltage sag, swell, interruption and harmonics. In the proposed method, colorized CWT coefficients of the voltage signals are applied to CNN as an image file. Experiments were conducted on a dataset containing 1500 real-life disturbance signals measured from different locations in Turkey by Turkish Electricity Transmission Corporation. This work is very similar to this research proposal, as it indicates how it is possible to achieve high accuracy with simple methodologies and robust techniques. Finally, the authors in Mishra, Subudhi e Jain (2019), Ahajjam et al. (2020) propose methodology similar to the last article is used, but it uses signals from mathematical functions. The results showed relevantly high accuracy.

These works make up the state-of-art related to the concepts and applications of this research. From them, it is possible to identify the advanced map so far and highlight the contributions that this work intends to bring. In the next sessions, the theoretical basis and research topics will be presented and discussed.

2.2 Smart Grid Integrated Perspective

The electric power system has undergone constant transformations. These changes are associated with an increase in renewables' penetration, the great revolution of ICTs, improvement of the computational performance capacity, search for sustainable infrastructures, and decentralization of power generation. The complexities pointed out several

times in this research become part of the different levels of electrical grids. New paradigms for the consumer's role, for market dynamics, and technical challenges to maintain the reliability of energy supply are emerging.

> Soon, our energy systems will change further. It is believed that large-scale power plants will be complemented by a large number of small scale energy generation units. Among others, individual households will generate solar or wind energy. It is also believed that intelligent systems will be used to communicate comprehensively, control, protect, and balance supply and energy demand. The whole structure of central and local energy generation, transmission and distribution, and enabling intelligent control and information systems is called a smart grid. Smart grids will be integrating microgrids (local systems) and super grids (high voltage transmission and bulk generation systems) (RIBEIRO; POLINDER; VERKERK, 2012).

The SG will spare no effort to guarantee a more reliable, sustainable, automated system proposal, characterized by the two-way flow of energy and information. It also has at its core, a broad application of measurement and integrated sensing. Grids must be able to have a quick response to undesired events, robust control strategies, and self-diagnostic capacity to overcome the barriers already mentioned. Below are some features associated with the SG concept (VIJAYAPRIYA; KOTHARI, 2011; U.S. Department of Energy, 2008; IEEE SA, 2013; KHUFFASH, 2018):

- Increased use of digital information and controls technology to improve reliability, security, and efficiency of the electric grid;

- Better facilitate the connection and operation of the traditional and distributed generation;

- Penetration and integration of distributed resources and generation, including renewable resources;

- Capable of meeting increased consumer demand without adding infrastructure;

- Usage of key technologies and applications to improve grid performance;

- Development and incorporation of demand response, demand-side resources, and energy-efficiency resources;

- Integration of smart appliances and consumer devices;

- Increasingly resistant to attack and natural disasters, with self-healing aspects;

- Capable of delivering power quality;

- Consider social aspects.

In this way, the new grid architectures appear to meet all these points. It is possible to divide the complexities of this new context into dimensional, technological, and stakeholders (RIBEIRO; POLINDER; VERKERK, 2012). Figure 2.1 illustrates this scenario of complexity. This understanding is essential to understand how the approaches that will be detailed in the next chapters bring SG contributions to PQ.
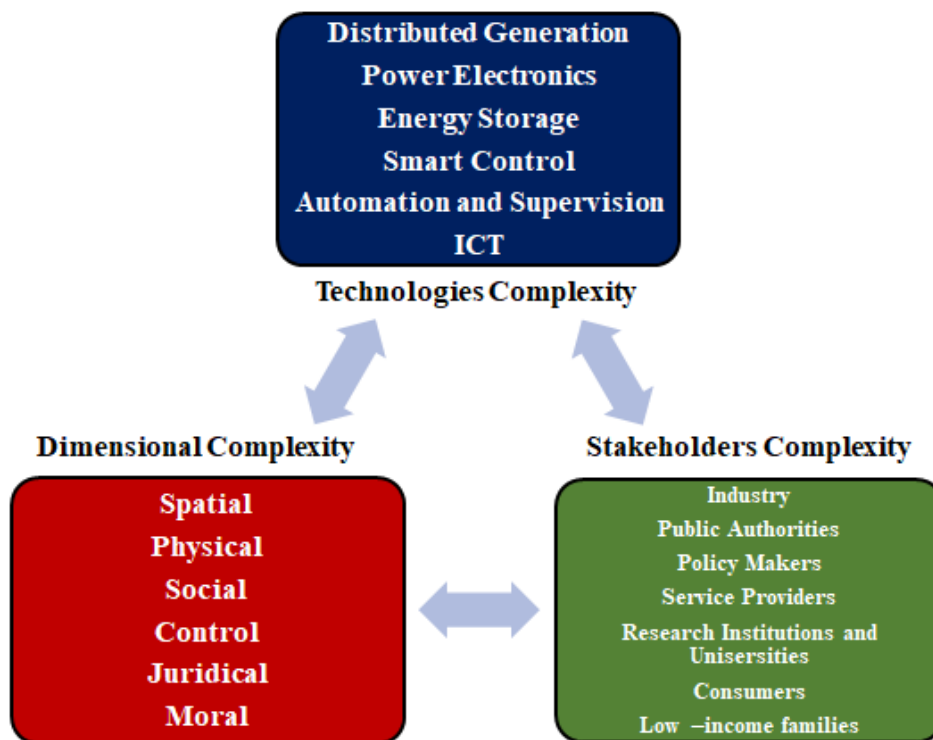
Figure 2.1 – Integrate perspective of SG complexity (Adapted from (RIBEIRO; POLIN-DER; VERKERK, 2012)).

2.3 Integrated Metrics of Quality Performance

The term PQ is used to describe the variation of the voltage, current, and frequency on the power system beyond a limit (JAIN, 2018). These variations are caused by grid disturbances and are not desired, as they can cause improper operation and damage to equipment, instability, damage to consumer equipment, among other concerns. It is practically impossible to eliminate the disturbances (KAZIBWE et al., 1990), but projects must be concerned with operating within the standards, in addition to measuring, and identifying these events.

The main factors influencing PQ are: generation equipment, end-user equipment and the grid itself (ZAVODA et al., 2018). In addition to the traditional sources (motors, transformers, nonlinear loads, etc.) of PQ issues, smart grids are mainly affected by the generation of emissions in the electrical networks by the power electronic converters interfaced with PV panels, electrical vehicle chargers, batteries, etc (RÖNNBERG; BOLLEN, 2016). With the modernization and changes in electrical power systems, it is increasingly necessary to use innovative methods to classify events involving voltage disturbances.

In the past, few disturbances were the focus of research. With new trends and even changes in traditional ones, there is a need for intelligent and integrated signal processing techniques to qualify better and treat problems. Figure 2.2 summarizes the context of the PQ disturbances, highlighting those investigated by this work. The option of select these classes, is associated with the desired frequency range for application of signal processing and limit the scope to simplify the modeling and data generation process.
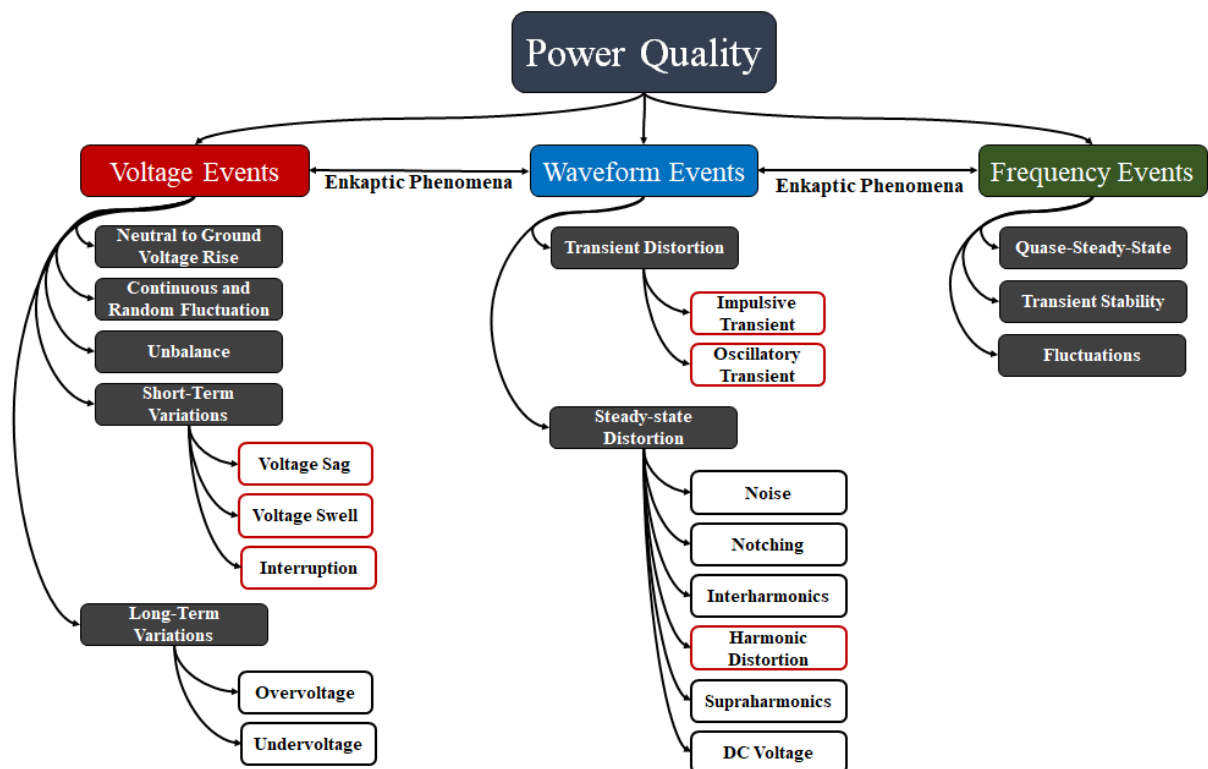
Figure 2.2 – Power Quality Context for Smart Grid.

The IEEE 1159-2019 standard (IEEE, 2019) establishes some definitions, characterizes and discusses some power quality disturbances. This material and other essential references were guided to model these events and base this research concept. This section aims to describe the events covered by this research. Table 2.1 resumes the disturbance parameters.

Table 2.1 – Features of investigated PQ voltage disturbances (IEEE, 2019).

Categories	Spectral	Duration	Magnitude
1. Transients			
1.1. Impulsive			
1.1.1. Nanosecond	5 ns rise	< 50 ns	
1.1.2. Microsecond	1 μs rise	50 ns - 1 ms	
1.1.3. Millisecond	0.1 ms rise	> 1 ms	
1.2. Oscillatory			
1.2.1. Low Frequency	<5 kHz	0.3-50 ms	0 - 4 pu
1.2.2. Medium Frequency	5-500 kHz	20 μs	0 - 8 pu
1.2.3. High Frequency	0.5-5 MHz	5 μs	0 - 4 pu
2. Short-term RMS variations			
2.1. Instantanous			
2.1.1. Sag		< 0.5 - 30 cycles	0.1 - 0.9 pu
2.1.2. Swell		0.5 - 30 cycles	1.1 - 1.8 pu
2.2. Momentary			
2.2.1. Interruption		0.5 cycle - 3 sec	< 0.1 pu
2.2.2. Sag		30 cycle - 3 sec	0.1 - 0.9 pu
2.2.3. Swell		30 cycle - 3 sec	1.1 - 1.4 pu
2.3. Temporary			
2.3.1. Interruption		>3 sec - 1 min	< 0.1 pu
2.3.2. Sag		>3 sec - 1 min	0.1 - 0.9 pu
2.3.3. Swell		>3 sec - 1 min	1.1 - 1.2 pu
3. Waveform distortion			
3.1 Harmonics	0 - 9 kHz	steady state	0–20%

2.3.1 Impulsive Transient

An impulsive transient is a sudden, unidirectional in polarity, nonpower frequency change from the nominal condition of voltage, generally characterized by peak value and duration times (IEEE, 2019). Lighting strikes are the most common causative events. It can hit any part of electrical system and damage equipment or connected loads from High Voltage (HV) and Low Voltage (LV) (RIBEIRO et al., 2013). This event's damaging effects can be immediate to the event or gradual (it deteriorates equipment materials over time) since the amplitude surge can generate several problems. Figure 2.3 shows a Impulsive transient waveform.

2.3.2 Oscillatory Transient

An oscillatory transient is a sudden, nonpower frequency change in the steady-state condition of voltage, with a bidirectional behaviour in polarity (IEEE, 2019). In other words, the instantaneous voltage or current value of an oscillatory transient varies its polarity quickly. "Oscillatory transients show a damped oscillation with a frequency ranging from a few hundred Hertz up to several megahertz" (BOLLEN; STYVAKTAKIS;

One Phase Oscillography
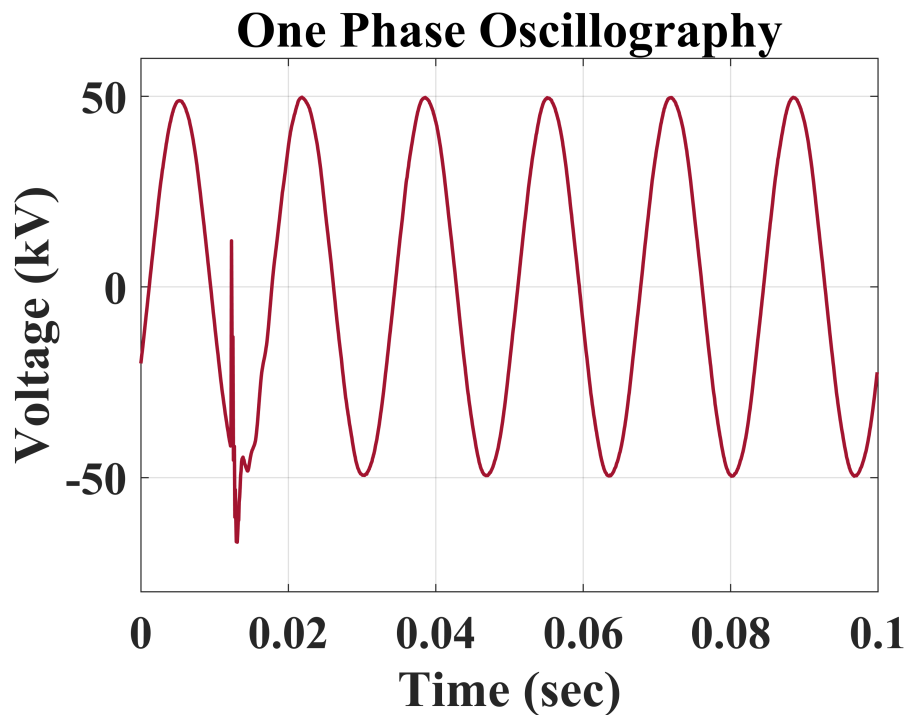
Figure 2.3 – Impulsive Transient in a Substation.

GU, 2005). A particular type of this event is the capacitor switching transient that begins with a negative transient followed by a positive transient of 1.2x to 1.8x the typical value of the sine wave, and then followed by an oscillatory transient of 400-2000 Hz standard, an endless quarter cycle or less (IEEE, 2019). Figure 2.4 shows a oscillatory transient waveform.

2.3.3 Voltage Sag

Voltage sag is a momentary decrease in voltage outside the typical tolerance. In IEEE 1159 2009 standard is defined as: "A sag is a decrease in RMS voltage to between 0.1 pu and 0.9 pu and duration from 0.5 cycles to 1 min" (IEEE, 2019). These can be caused by a heavy motor starting, faults and also heavy load changes or switching. Figure 2.5 shows a voltage sag waveform. The effects related to this disturbance are "malfunctions of electronic drives, converters and equipment with an electronic input stage, relays and contractors can drop out, and asynchronous motor can take a current higher than its starting current at recovery process" (MORENO-MUÑOZ, 2007).

2.3.4 Voltage Swell

Swell is the opposite of sag, a short duration phenomenon of increase in RMS voltage between 1.1 and 1.8 pu, and duration of the event ranges from 0.5 cycles to 1 min. Swells are rare events as compared to sags (CHATTOPADHYAY; MITRA; SENGUPTA,
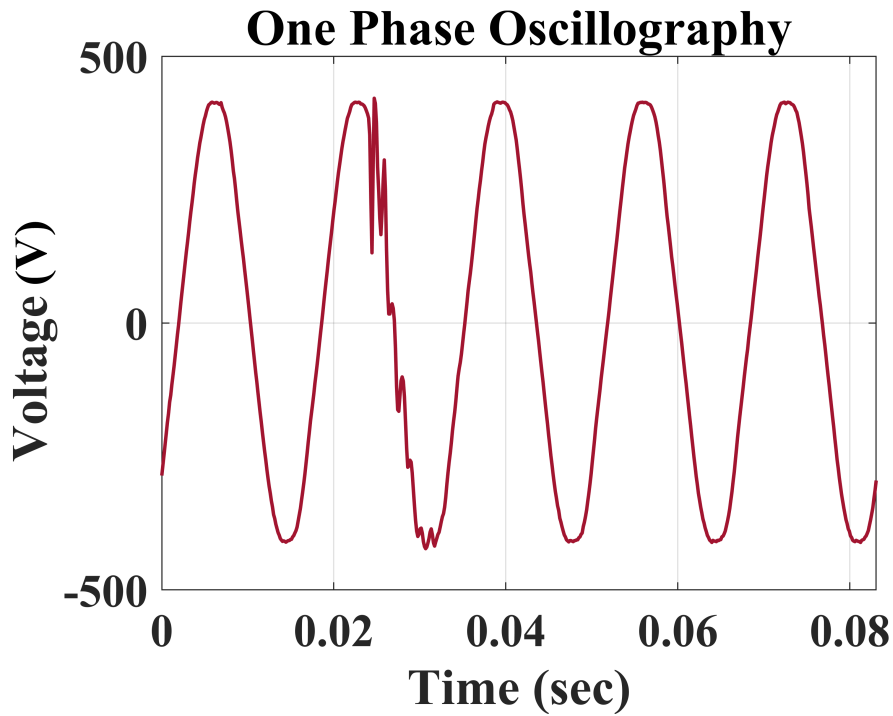
Figure 2.4 – Oscillatory Transient in a Distribution System.
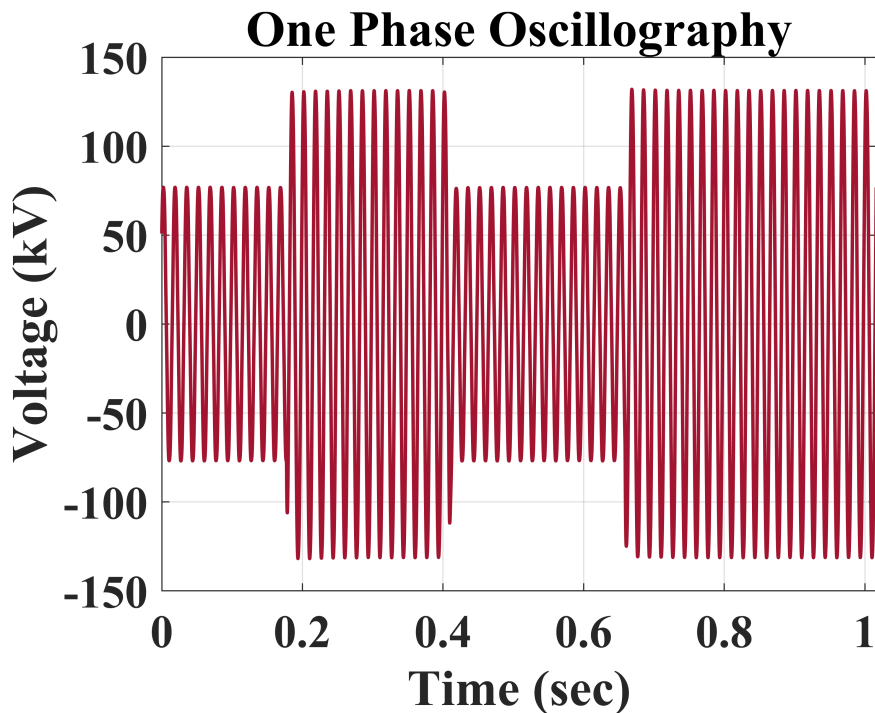
Figure 2.5 – Voltage Sag in a 88 kV Medicine Facility.

2011). Swells are more difficult to occur when compared to sags. This disturbance are normally associated with fault conditions and can also be caused by switching off a large load and load shedding (IEEE, 2019). The effects are similar to sags, and also can trip-out protection circuits of power electronics. Figure 2.6 shows a voltage swell waveform.
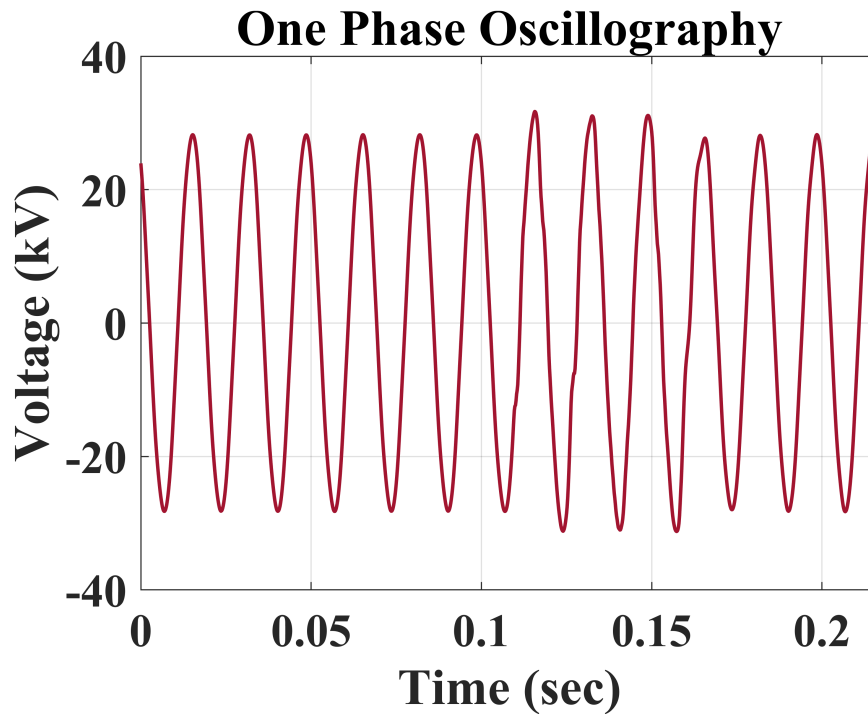
Figure 2.6 – Voltage Swell in a 34 kV Iron Mineration Facility.

2.3.5 Interruption

Interruption is defined as a reduction in the supply voltage, or load current, to a level less than 0.1 pu for a time of not more than 1 minute, that can be caused by system faults, equipment failures or control and protection misoperation (IEEE, 2019). As it is also a short-term variation of the voltage RMS, the expected effects are the same as those of sag, with worsening due to drastic reduction. Figure 2.7 shows a interruption waveform.

2.3.6 Harmonics

Harmonics are periodic sinusoidal distortions of the supply voltage or load current, and are measured in integer multiples of the fundamental supply frequency of 50/60 Hz (COLLINSON; STONES, 2001). The electronic-based equipment is a significant source of harmonics in power systems, like rectified input, switching power supplies, and also nonlinear loads (IEEE, 2019). In smart grids context, with the extensive penetration of renewables that are based on equipment with this emitting characteristic, harmonics continue to be the object of concern and research, both in the academic environment and in the industry. Harmonics are common in the power systems and can be observed in measurements. The grid operator concern is always to keep the level within the recommendations of the standards and grid codes. Figure 2.8 shows a voltage waveform with harmonics. The main harmonic effects are (WIECHOWSKI, 2006; DUGAN et al., 2012; HAMEED; YOUSAF; Khan Sial, 2016):

One Phase Oscillography
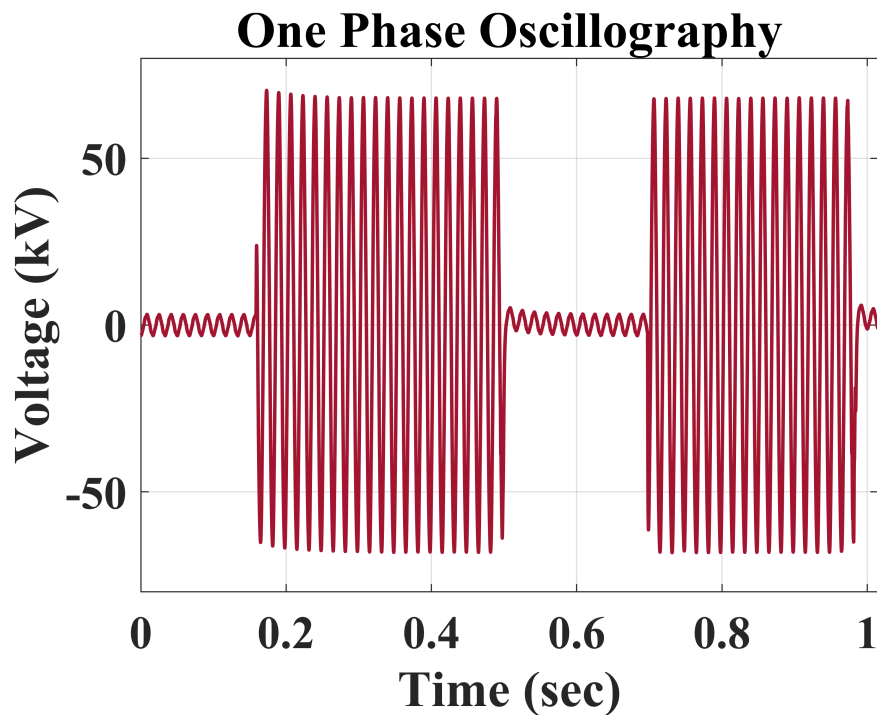
Figure 2.7 – Interruption in a 88 kV Medicine Facility.

- The possibility of amplification of harmonic levels resulting from series and parallel resonances;

- Degradation of the power factor;

- Overheating of the phase and neutral conductors;

- Efficiency of the generators is reduced day by day due to harmonics;

- Eddy current and hysteresis losses in transformers;

- Overheating of the system components e.g. generators, motors and transformers etc;

- Interference problem with telecommunication ;

- Developed disturbing moments and noise in rotating machines;

- triplen harmonics may overload neutral conductor in LV networks;

- Among others.

2.4 Signal Processing Framework

This session will cover signal processing, both the advanced framework and the concepts involving CWT and scalograms. These points are essential to substantiate what research proposes for development.
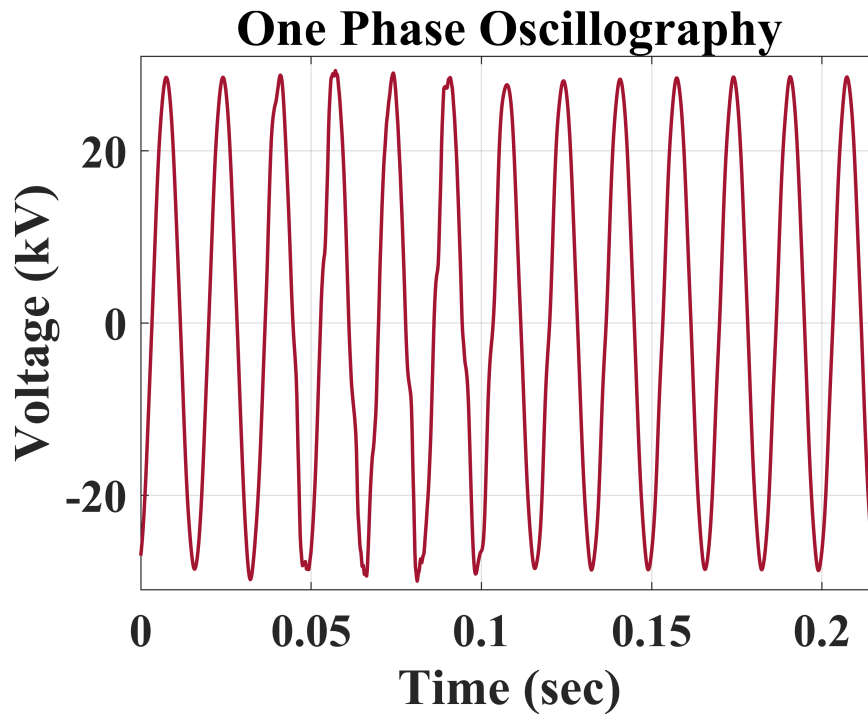
Figure 2.8 – Harmonic Distortion in a 34 kV Iron Mineration Facility.

2.4.1 Advanced Signal Processing for Power Systems

The use of signal processing in power system applications is widespread. Analysis of the signals measured in the electrical grid is of paramount importance for the proper functioning, guaranteeing the quality and reliability of services. For this, the measurement aspects and characteristics of each voltage/current signal must be well known for the effective use of the techniques.

Measurement and analysis of signals at different points in the system allow the complete assessment of the grid condition (RIBEIRO et al., 2013). The rising of complexity in power systems requires a wide and comprehensive signal monitoring together with the suitable signal processing for characterizing, identifying, diagnosing, protecting, and also for better unfolding the nature of certain phenomena and events (SILVA; DUQUE; RIBEIRO, 2015). In the context of SG, where there is a philosophy of mass measurement and sensing for all levels of power systems, the advanced signal processing leads as one of the tools that can enable several other applications. It is reflected in the various fields of this new network structure: communication, control, protection, automation, operation, power quality, etc. Figure 2.9 shows the general application scheme for advanced signal processing and highlights this work scope.

The results that can be obtained through signal processing have a variability of utility and applications in power systems. Also, the different techniques that can be applied generate a range of results as well. SGs can take full advantage of these aspects
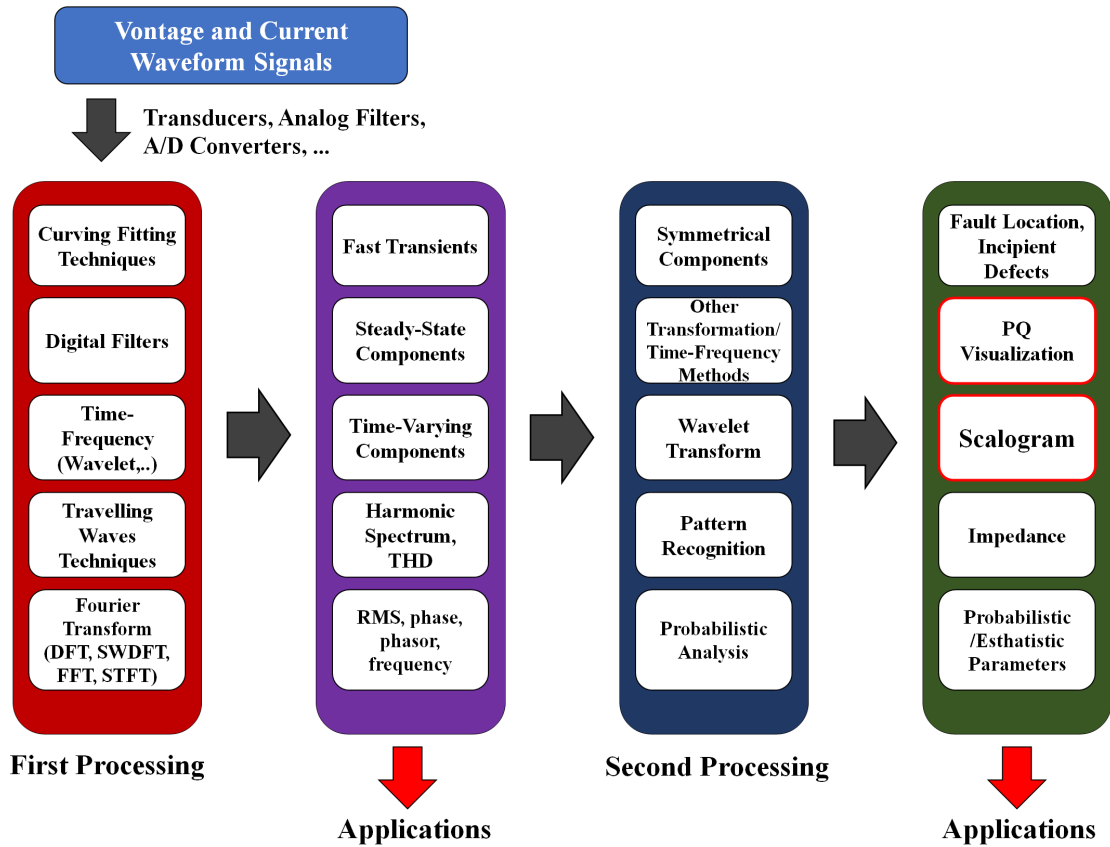
Figure 2.9 – General application scheme for advanced signal processing (Adapted from (RIBEIRO et al., 2013)).

to improve identification, characterization, and analysis. The advanced SP uses various types and domains, allowing you to choose the one that best fits the application.

The smart grid of future will require not only advanced signal processing for identification of parameters but also intelligent methods and assessment for identifying particular patterns of behavior (RIBEIRO et al., 2013). In this way, pattern recognition becomes a powerful application for power system diagnostic and monitoring solutions. Given this, several classification methods use signal processing for feature extraction of signals. The techniques based on wavelets present satisfactory results for this type of application, besides being widely used.

2.4.2   Continuous Wavelet Transform (CWT)

"Wavelet transform is known as a mathematical microscope, which provides a multiresolution analysis of the data under consideration" (GHAREKHAN et al., 2010). The CWT allows the analysis of non-stationary signals at multiple scales and uses a window to extract signal segments. The window is called a wavelet (SHOEB; CLIORD, 2006). For comparison, CWT is a generalization of Short-Time Fourier Transform (STFT) to overcome the resolution limitations. In this transformation, it is possible to shorten or

lengthen the window depending on the wavelet scale, besides the translation. In that case, the lower the scale, the greater the sensitivity to variations in frequency. The 2.1 describes CWT.

$$C(a,\tau) = \int \frac{1}{\sqrt{a}} \Psi(\frac{t-\tau}{a}) x(t) dt \qquad (2.1)$$

Where C is the transformation, a is the scale factor, τ is the translation time, Ψ is the mother wavelet function and $x(t)$ is the input signal in fuction of time.

When the wavelet is contracted (a smaller then 1) the wavelet offers high spectral resolution, when the wavelet is dilated (a bigger then 1) the wavelet offers high temporal resolution. In the first case, it is ideal for transient events, while the second is ideal for determining frequencies in phenomena in steady-state.

The main properties that the wavelet function must obey are that of finite energy and the admissibility condition. These are described in the equations 2.2 and 2.3, respectively.

$$E = \int_{-\infty}^{\infty} |\psi(t)|^2 dt \qquad (2.2)$$

$$\int_{-\infty}^{\infty} \psi(t) dt = 0 \qquad (2.3)$$

Where E is the energy of the wavelet and Ψ is the wavalet mother function.

The graphical representation of the correlation between the signal and the wavelets scaled over time is called a Scalogram. The CWT automatically adjusts its time and frequency resolution depending of activity by dilating or contracting the analysis window (SHOEB; CLIORD, 2006). It is a time-scale representation with the distribution of the signal's energy and expressed in power per frequency unit, just like a spectrogram (RIOUL; VETTERLI, 1991). The scalogram of the signal "$x(t)$, is defined by 2.4. Fig.2.10 shows one example of a scalogram generated in MATLAB.

$$S(a,\tau) = |C(a,\tau)|^2 \qquad (2.4)$$

The multiresolution analysis of CWT can be computed through a filter bank, these are a set of filters that compose the signal in specific frequency ranges. Fig. 2.11 illustrates a scheme of filters associated with three levels. The low-pass and high-pass filtering branches of compute respectively the approximations and details of the signal x(k), which is the sampled signal. For a special set of filters L(z) and H(z) this structure is called the DWT, the filters are called wavelet filters (MERRY, 2005).
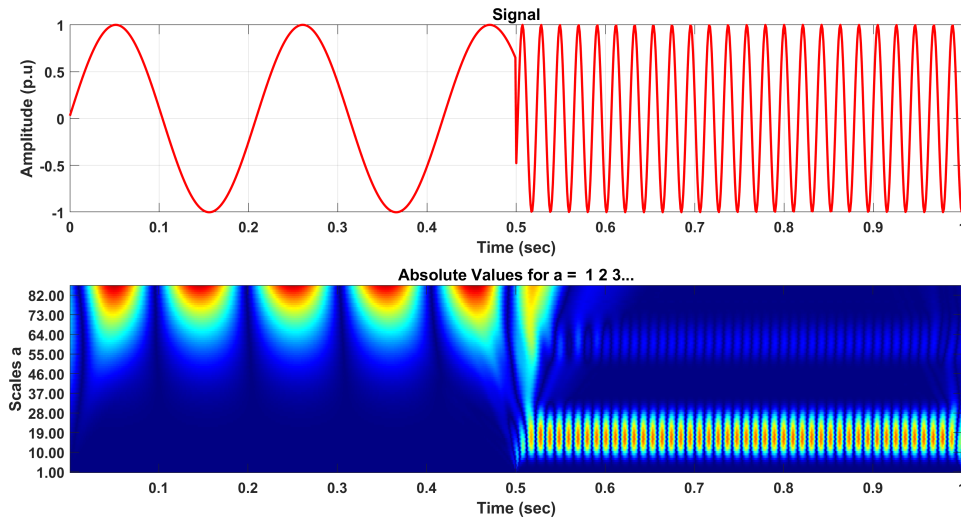
Figure 2.10 – Example of scalogram generated in MATLAB.
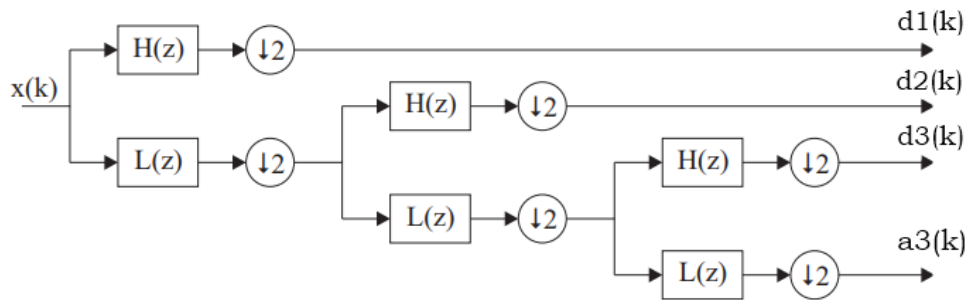
Figure 2.11 – A three level bank filter scheme.

In this work, the CWT method with filter banks is performed to extract, through time-frequency analysis, a 2-D representation of the voltage signals. These representations will allow differentiating the events by an image with DL techniques, subject to be addressed in the following section, for pattern recognition and classification. For power system electromagnetic transient signals, the wavelet basis should have two desirable characteristics (GALLI; HEYDT; RIBEIRO, 1996): reduce the number of wavelet components that describe the signal, and reveal the natural transient oscillatory components of the signal.

In references (MERRY, 2005; RIOUL; VETTERLI, 1991; PERCIVAL; WALDEN, 2000), it is possible to find a more in-depth approach to the subject, with all the details and which also served as a guide and basis for the concepts described here.

2.5 Deep Learning Framework

In this part of the text, the framework involving AI and DL is presented. Thus, intertwined concepts are also raised and are essential for the flow of research.

2.5.1 Deep Learning and AI

AI is the term used to attribute machine knowledge, which emulates human mental skills and activities, such as perception, understanding, learning, behavior, decision-making, etc (KIM, 2020). It can also be described as the ability of a computer algorithm to perform the human brain. From this concept, several sets of methods, models, and algorithms are used in different applications, including power and energy systems. The branches that involve this subject are Natural Language Processing, Robotics, Expert Systems, Fuzzy Logic, Machine Learning (ML), and DL.

ML is a technique for studying and analyzing data, learning from large databases, and making decisions based on learning. A key feature of ML is an iterative method to learn from previous computations and adapt independently (KIM, 2020). DL, on the other hand, is a subset of ML that uses a neural network model. The latter is one of the important objects of the research developed, and in this aspect, that will be focused. Figure 2.12 shows the set of methods associated with ML and where DL is inserted. Within ML, there are three types of learning: supervised, unsupervised and reinforcement. It will separate the kinds of methods and techniques used for specific applications. Below is the explanation of each kind:

- **Supervised:** These algorithms have prior learning based on a system of labels associated with data, which allows them to make decisions, predictions or classifications.

- **Unsupervised:** These algorithms have no prior knowledge. They deal with massive lawlessness data sets, intending to find patterns that will somehow allow them to be organized.

- **By reinforcement:** The algorithm learns from experience itself. That is, making the best decision in different situations according to a trial and error process in which the right choices are rewarded.

DL is a set of algorithms in machine learning that attempt to learn in multiple levels, corresponding to different levels of abstraction, it is typically used to abstract useful information from data (CHEN, 2015). It is an AI technique that has been implemented for several years to classify images, text, data or sound. DL is usually implemented using a neural network architecture, and the term "deep" refers to the number of layers in the network, so more layers mean a deeper network (MATHWORKS, 2020). The number of layers of this type of network can reach more than a hundred. Common DL techniques include CNNs and Long Short-Term Memory (LSTM) (it is recurrent neural network). The neural networks architecture are a combination of multiple nonlinear processing layers and are inspired by biological nervous systems (MATHWORKS, 2020d). It kind of models can achieve high levels of accuracy in object classification, sometimes can overstep human-level
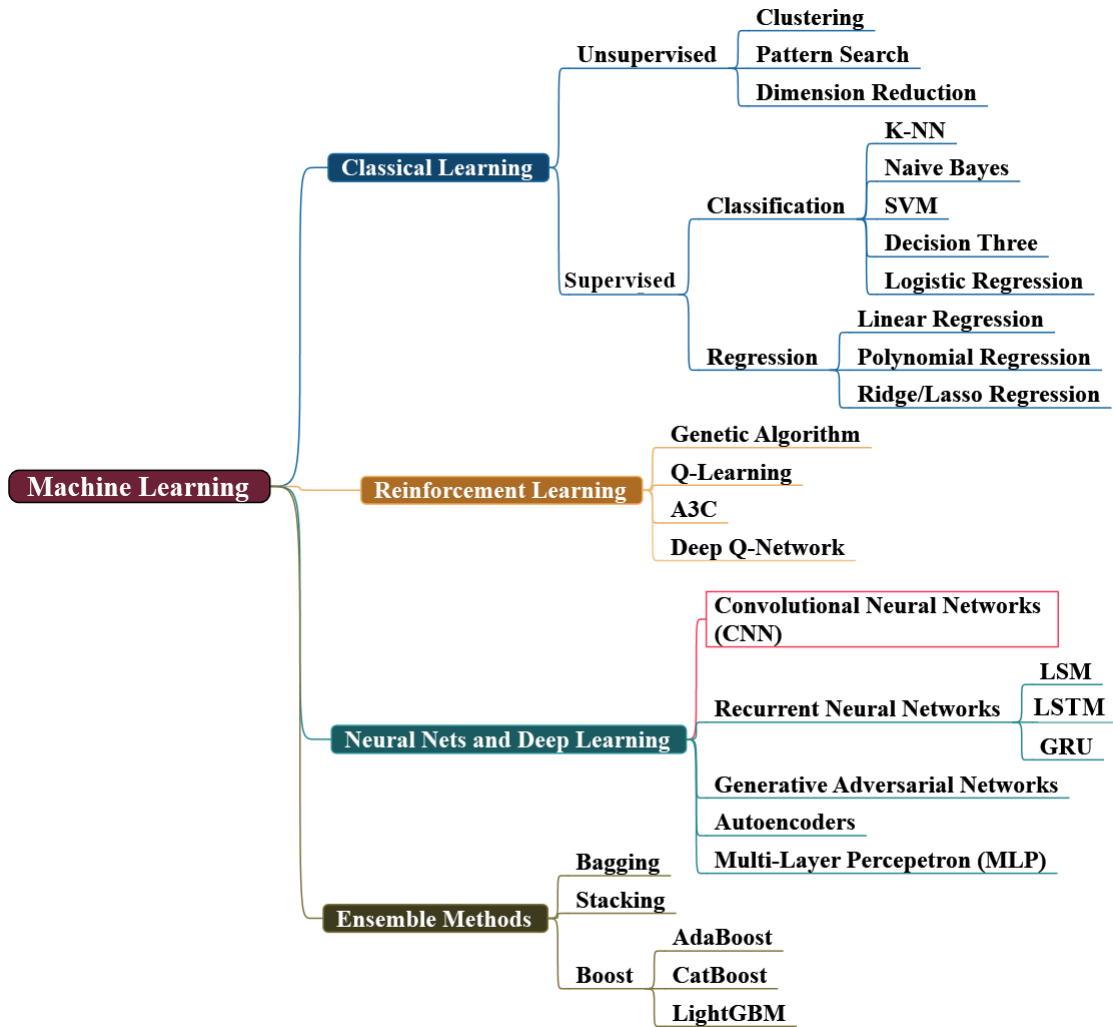
Figure 2.12 – Machine Learning examples of methods highlighting DL research application.

performance (BEALE; HAGAN; DEMUTH, 2020). Figure 2.13 show the main differences between DL and ML.
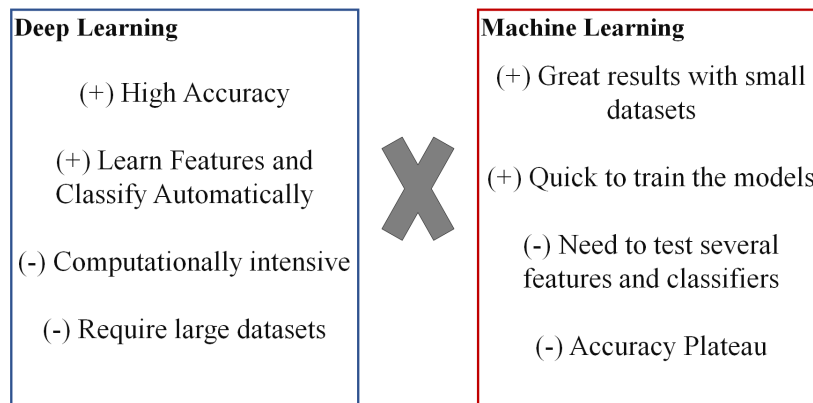
Figure 2.13 – Comparing advantages and disadvantages of DL and classical ML classification methods .

The techniques involving ML, including DL, can be applied for classification, regression/forecasting, and clustering. The use ranges from more straightforward applications such as games to even cutting-edge smart technologies, such as robotics and aviation. In electrical power systems, mainly in SG, these techniques are taking on an important role and will become even more essential for the future network. With the decentralization of systems and the massive flow of data, AI is critical for a reliable, safe and automated performance. Below are listed some DL applications for power systems (OZ-CANLI; YAPRAKDAL; BAYSAL, 2020; MISHRA et al., 2020):

- Load forecasting;

- Wind, Hydro and Solar generation forecasting;

- PQ disturbances classification;

- Islanding detection in distributed generation systems;

- Fault type classification;

- Fault location;

- Fault diagnosis for equipments;

- Cybersecurity in SG;

- Theft of electricity in SG;

- Optimization o renewable energy resources;

- Microgrid Energy Management Systems;

- Control and Automation;

- Among others.

In this research, DL is used to classify PQ disturbances employing neural networks of deep layers. In the next session, the subject and the type of network will be deepened. Training deep layered neural networks is considerably and time-consuming and requires a great deal of computational strength. Also, a significantly large data set is needed. On the other hand, developer interference is minimal, and accuracy can reach unlimited levels.

> With few assumptions and little manual interference, structures similar to the hierarchical cone are being automatically learned from large amounts of data. These learning approaches are especially interesting in that, because they learn, they are not fixed for

any specific task, and they can be used in a variety of applications. (ALPAYDIN, 2016)

Two methods of development will be considered, design from scratch and transfer learning. The first is creating the network from scratch and training it appropriately for a specific task. The other method uses a pre-trained network (with a similar propose) for reuse with a new data set and classification. It allows less use of labeled data for training and reduces commuting effort. In (MATHWORKS, 2020b), the process to achieve the transfer learning is explained:

1. Select a relevant network that has been trained for a task similar to the new task;

2. Replace the classification layers for the new task. If a large dataset is available, it is possible to tune other layers without overfitting;

3. Train the network on the data for the new task;

4. Test the accuracy of the new model.

2.5.2 Convolutional Neural Networks (CNN)

CNN is used as a DL method to classify images with scolagrams that describe the signal with voltage disturbance. CNN is feed-forward neural networks that use a spatial-invariance trick to learn local patterns, most commonly, in images efficiently (LÓPES et al., 2019). CNN is specially designed considering the structure of images. The input and output of each stage of a CNN are called feature maps (WANG, 2016). For the first block, the input is an image, so each block's output is a feature extraction of the input. It consists of three types of layers: convolutional layer, activation layer, and pooling layer. The last block is a fully connected layer which outputs predictions on classes. Fig. 2.14 shows an illustration of a typical CNN's architecture.
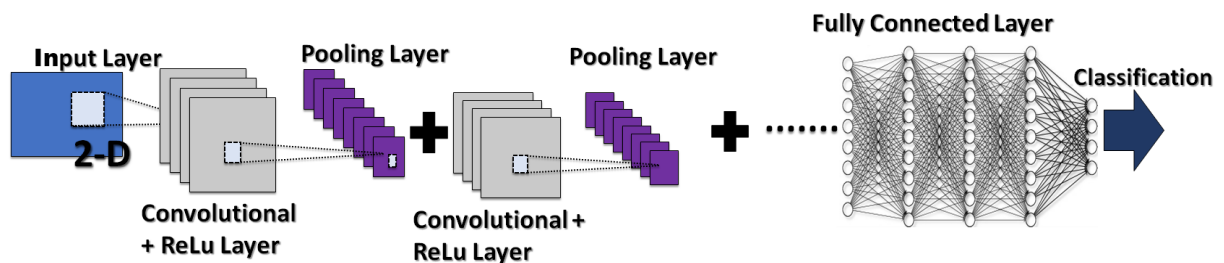
Figure 2.14 – CNN typical architecture.

Several architectures and combinations can be implemented, the most common being serial arrangements and an arrangement Directed Acyclic Graph (DAG). A DAG network can have a complexity layout in which layers have inputs from multiple layers and

outputs to various layers. The series architecture, on the other hand, provides a simple and direct line of connections. The most common layers in the literature are described below:

- **Convolutional Layer:** A convolutional layer is the main component of a CNN that contain a set of convolutional kernels (filters) which generate an output feature map by convoluting with a given input (KHAN et al., 2018). When placing the input image through these filter sets, each activates a feature of the image. As you pass the consecutive convolutional layers, the size of the filters normally increases. The equation 2.5 describes the output of the convolutional layer.

$$y_j^k = \sum_i W_{ij}^k * x_j^k + b_j^k \tag{2.5}$$

  Where y_j^k is the output feature map, x_j^k the imput feature map, W_{ij}^k is the set of 2-D filters and b_j^k is the trainable bias parameter.

- **Rectified Linear Unit or ReLU Layer:** It is an activation function that maps negative inputs to 0. Despite the simplicity of the procedure, it is one of the most used as far as the author knows due to its operating speed. The equation 2.6 describes the ReLu function.

$$f_{relu}(x) = max(0, x_r) \tag{2.6}$$

  Where x_r is the funciton input and max is a syntax for ramp funcion.

- **Pooling Layer:** Pooling uses nonlinear downsampling to simplifies the output, reducing the number of learning parameters. The size of the output feature map from an max-polling is given by equation 2.7.

$$h_r = max_1^{MxM}(x_{pj}) \tag{2.7}$$

  Where h_r is the output feature map, x_{pj} is the element of the pooled region X_{pr} and M is the pooled region's dimension size.

- **Fully Connected Layer:** "Correspond essentially to convolution layers with filters unit size filters, where each unit in a fully connected layer is connected to all the units of the previous lay" (KHAN et al., 2018). The equation 2.8 describes the layer.

$$z = f(W^T q + b) \tag{2.8}$$

  Where where q and z are the vector of input and output respectively. W denotes the matrix with the connections weights, and b represents the bias term vector.

- **Classification Layer:** "A classification layer computes the cross-entropy loss for multi-class classification problems with mutually exclusive classes" (BEALE; HAGAN; DEMUTH, 2020).

To perform the stages of the study of DL and CNNs, the Deep Learning Toolbox in MATLAB was used, which contains several specific tools that help in the development. Therefore, when dealing with optimization algorithms for deep-layer neural networks, attention is paid to the Stochastic Gradient Descent (SGD).

> SGD performs a parameter update for each set of input and output that are present in the training set. As a result, it converges much faster compared to the batch gradient descent. Furthermore, it is able to learn in an "online manner", where the parameters can be tuned in the presence of new training examples. The only problem is that its convergence behavior is usually unstable, especially for relatively larger learning rates and when the training datasets contain diverse examples. When the learning rate is appropriately set, the SGD generally achieves a similar convergence behavior, compared to the batch gradient descent, for both the convex and non-convex problems (KHAN et al., 2018).

Momentum-based training optimization improves SGD with great convergence, besides solving the delay in the update due to fluctuations (KHAN et al., 2018; MURPHY, 2012). This method is applied in this research and the equation 2.9 describes the algorithm. Other algorithms such as RMSProp and Adam can also be used, in the references (KHAN et al., 2018; MATHWORKS, 2020b) presents in greater detail.

$$\theta_{\epsilon+1} = \alpha \nabla E(\theta_\epsilon) + \gamma(\theta_\epsilon - \theta_{\epsilon+1}) \tag{2.9}$$

Where is ϵ the iteration number, α is the learning rate, α is the parameter vector, and $E(\theta)$ is the loss function.

In reference (KHAN et al., 2018) and (KIM, 2017), will find more comprehensive details and other alternatives associated with the design and development of CNN for various types of application as well. And also CNN architectures for transfer learning.

2.6 Considerations

This chapter presents an overview of the main theoretical tools that will feed the theoretical basis for the explicit development of Chapter 3. Some references were

given to point out more details about the concepts that have been well described and contextualized with the problem.

3 Research Procedures and Development

This chapter describes the procedures and stages of development. First, the method and model used to generate power quality signals will be detailed. Soon after, a brief description and illustration of scalograms extraction from the signals in a way that characterizes them. Finally, the CNN design, choice, and braking procedures are detailed.

3.1 Data Generation

The generation of the data signal is one of the fundamental steps to carry out this research. As models based on DL require large amounts of data for excellent training performance, experts recommend in the ranges of thousands, at least. For that, the MATLAB Simulink tool was used. Through the Specialized Power Systems (Simpowersys) library of Simscape Electrical, a 220 kV transmission system was modeled based on the IEEE 5 bus benchmark system's topology. This tool allows the user to use a library with specialized models for power systems with load components, transmission lines, generation, among many other equipment and devices. A particular series of analyses for the power system can also be used and generate common events such as faults, load switching, or capacitor bank. The variety and possibility are tremendous, and the use among professionals and researchers in the area is recurrent. Figure 3.1 shows the modeled system.
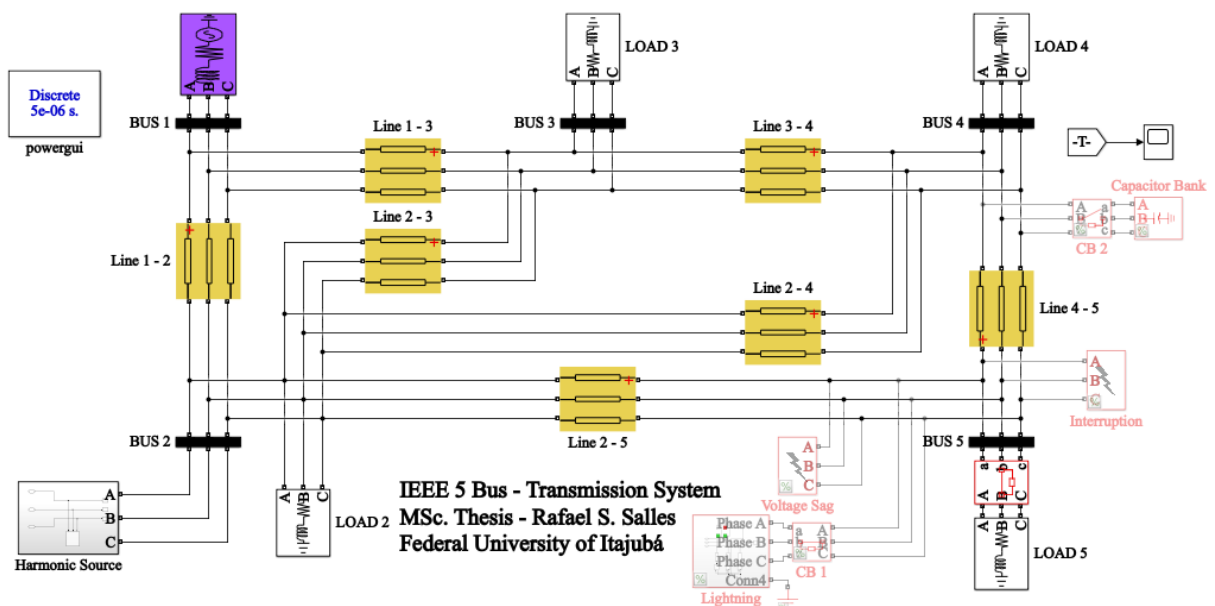
Figure 3.1 – 220 kV Transmission System in Simulink.

The purpose of using a reference system and typical network values is to get the signals generated from reality closer to those found in the field measurement. Thus, despite

the system being based on the IEEE 5 Bus, the transmission line parameters were removed from (Val Escudero et al., 2019). The 220 kV OHL parameters are detailed in the Table 3.1.

Table 3.1 – 220 KV OHL Parameters.

Parameter	Data
Phase Conductors	600ACSR Curlew
Conductors per Phase	1
DC Resistance	$0.05527\ \Omega/km$
GMR	$12.75733\ mm$
Outer Radious	$15.8115\ mm$
Inner Radious	$4\ mm$
Shield Wires	None
Phase A Co-ordinates	$(-8.05,16.4)\ m$
Phase B Co-ordinates	$(0,16.4)\ m$
Phase C Co-ordinates	$(8.05,16.4)\ m$
Phase Transposition	Yes (perfectly symmetry)
Soil Resistivity	$400\ \Omega.m$

With these parameters, the application "Compute RLC parameters" is powered and can generate RLC parameters of overhead transmission line from its conductor characteristics and tower geometry. The results obtained as positive-sequence, zero-sequence, and mutual zero-sequence parameters of the transposed line were used. All the details and math behind the tool can be found at (MATHWORKS, 2020a). For the transmission line model, the "Distributed Parameters Line" was used. Table 3.2 shows the block parameters.

Table 3.2 – Distributed Line Parameters block values.

Parameter	Value
R1	$0.018441\ \Omega/km$
R0	$0.19244\ \Omega/km$
L1	$0.83262\ mH/km$
L0	$3.9161\ mH/km$
C1	$0.1395\ pF/km$
C0	$7.2246\ pF/km$

The other parameters of the system, such as distance between bars, and load power, are described in Table 3.3, and inspired in (BHANDAKKAR; MATHEW, 2018). The 220V voltage source on bus 1 has the ratio X/R = 7, 60 Hz of fundamental system frequency, and Short Circuit Level is 3000 MVA. The bar was configured for the "swing" type.

In Figure 3.1, it is possible to see the blocks connected in busbar 5. They are with half transparency in the Figure. Each block of this generates a PQ disturbance, one per

Table 3.3 – Line Lengths and Loads.

Line Length (km)	
1-2	47
1-3	87
2-3	67
2-4	67
2-5	47
3-4	19
4-5	87
Load Power	
Bus 1	-
Bus 2	20 MW / 10 MVAR
Bus 3	45 MW / 15MVAR
Bus 4	40 MW / 5 MVAR
Bus 5	60 MW / 10MVAR

batch of simulations to generate the investigated signals. With bus 5 measurements, the training data set for CNNs is generated. The test set, on the other hand, was developed using bus 4 as a reference. When combining a MATLAB script with the Simulink model, through a loop and random variations (normal distribution) in critical parameters that qualify voltage disturbances, different signals of the same class were obtained. The list below describes how the disturbance was generated and critical parameters changed in each simulation.

- **Oscillatory Oscillatory**: A heavy capacitive load was placed in bus 4. And through a switch, this capacitor bank is connected. The average value of Capacitive Reactive Power is 1.5 MVAr with 250 kVAr of variance.

- **Impulsive Transient (Lightning Surge)**: An electrical discharge was applied in busbar 5 with microsecond duration, in order to simulate a lightning. The average value of voltage discharge is 100 kV with 20 kV of variance.

- **Voltage Sag**: For this event, line to line fault was applied, at busbar 5. The parameter that creates randomness is the fault resistance value, which presents an average value of 20 Ω with a 10 Ω variance.

- **Voltage Swell**: The bus 5 load is disconnected and reconnected through a switch breaker. The variant parameters to generate the randomness is the load active power, with an average value 100 MW and 30 MW variance.

- **Interruption**: A three-phase fault to ground was performed in bus 5 with low fault resistance. The average value in loop simulation was 3 Ω with variance of 0.5 Ω.

- **Normal operation with harmonics**: The variant parameters to generate the randomness is the load active power, with an average value 100 MW and 30 MW variance.

Some harmonic current orders (5th, 7th, 11th, and 13th) were injected at busbar 2 through current sources and an associated parallel impedance to characterize the harmonics in the network, which is common in the real system.

The simulations loop for the training group was 200 iterations for each disturbance. The loop for the test set was 50 iterations for each disturbance. The codes used to perform this step can be found in Appendix B. With the generated signals, more signals were created with typical characteristics of real measurements, including noise. For each PQ issue class, the data set will receive three noise levels in Signal to Noise Ratio (SNR): 30, 40, and 60 SNRdB. That is, the training set at the end had 4800 signals, and the test set 1200.

3.2   Feature Extraction

After generating, verifying, and collecting the data, the next step is to create the scalograms from the obtained signals to characterize voltage disturbances. For this, tools from the MATLAB wavelet toolbox were used. The methodology for visualizing these events in 2-D images was to use this time-frequency representation to highlight the increase in frequencies above the fundamental during the investigated events. Scalograms are adequate because they can highlight the increase in energy associated with a specific frequency, containing time information.

The CWT with a filter bank has been ideal since the first attempts. It is possible to define the frequency range to investigate and employ facilitating algorithms within MATLAB. The script with the code for this step is in Appendix B. The algorithm used implies the CWT with a filter bank. The input parameters used are Sampling Frequency, Signal Size, Wavelet Type, Voices per Octave, and Frequency limits. Table 3.4 illustrates the values used in this work.

Table 3.4 – CWT Filter Bank Parameters.

Parameter	Value
Sampling Frequency	200 kHz
Wavelet Type	Generalized Morse Wavelet
Voices per Octave	48
Frequency Limits	[100 2000] Hz

The functions designed to obtain CWT with a filter bank allow the use of the analytical wavelet family. These are Generalized Morse Wavelet, Analytic Morlet (Gabor)

Wavelet, and Bump Wavelet. The number of voices per octave to use for the CWT, specified as an even integer from 4 to 48. The CWT scales are discretized using the set number of voices per octave. The energy spread of the wavelet in frequency and time automatically determines the minimum and maximum scales. The parameters chosen to generate these scalograms were based on the author's experience and on a set of attempts to show the increase in energy for frequencies above 100 Hz associated with voltage disturbances.

From the coefficients generated by the CWT to analyze the signal, Colour maps of the "jet 264" style available in MATLAB were assigned so that it was possible to observe the energy scales in the scalograms. This process is applied to the absolute value of the coefficients. Figure 3.2 shows the images for each disturbance.

Through this extraction in the time domain, it is also possible to visualize the expected differences when adding noise to the signals. With this, we will assess whether the proposed classifiers will achieve good accuracy even in noise signals. Figure 3.3 shows an example of the difference in images when adding noise.

Finally, after generating all the images, containing only the scalograms, they were saved in specific folders for each PQ disturbance class. The size of the saved images was 240x240 and in the "png" format. For this, the command "imwrite" and a support code were used to save many images.

3.3 CNNs Methods and Training

In the DL models' training stage, two methodologies were chosen, design and training CNN from scratch, the concept discussed earlier on transfer learning. In the first, the author's literature and previous experiences were used as a reference, but an analysis of performance during training determined the choice. The objective was to guarantee 100% accuracy on this stage and then proceed to the test stage. In this way, some training parameters were put to the test, and finally, a network model was chosen for the testing stage. The second method sought to determine three pre-trained CNNs available in MATLAB's Deep Learning Toolbox. In (MATHWORKS, 2020a) and in every MathWorks interaction community, it allows immersion in the topic and the use of the software. Due to the programming scripts available in Appendix B, training all networks was carried out.

In the case of pretrained networks, it was enough to replace the last layers to suit the proposed problem, as described in Chapter 2. The fully concealed layer and the classification layer were parameterized suitable for only six classes. Some directions were defined to choose the networks: different accuracy of each original model, varied computational effort and availability. The following networks were selected: SqueezeNet,
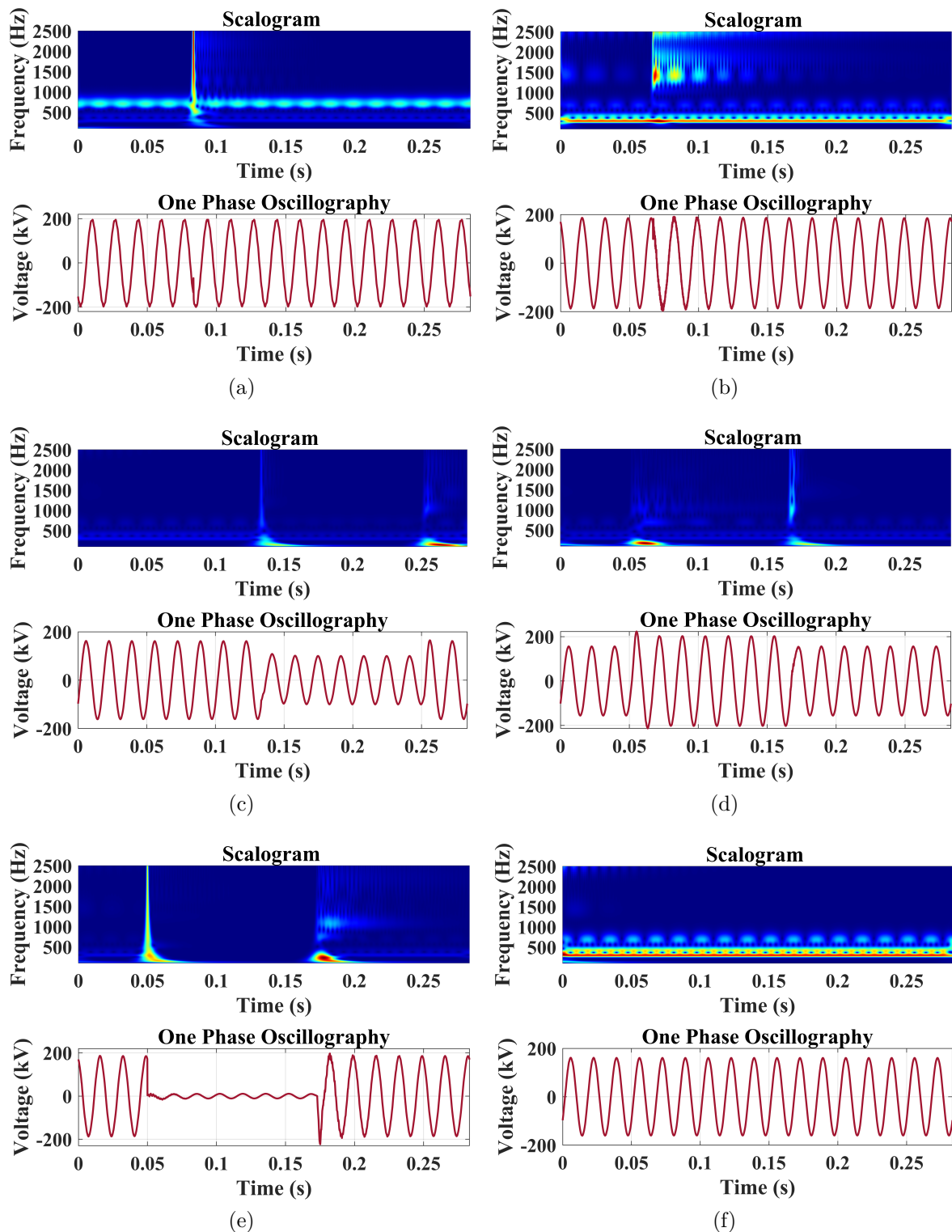
Figure 3.2 – Scalograms and Oscillographies of PQ disturbance: Impulsive Transient (a), Oscillatory Transient (b), Voltage Sag (c), Voltage Swell (d), Interruption (e), and Normal with Harmonics (f).

GoogleNet and ResNet-50. The first has less accuracy and less computational spend on training. The second presents a computational effort slightly more significant than the first and also accuracy. The ResNet-50 model, on the other hand, has higher accuracy but
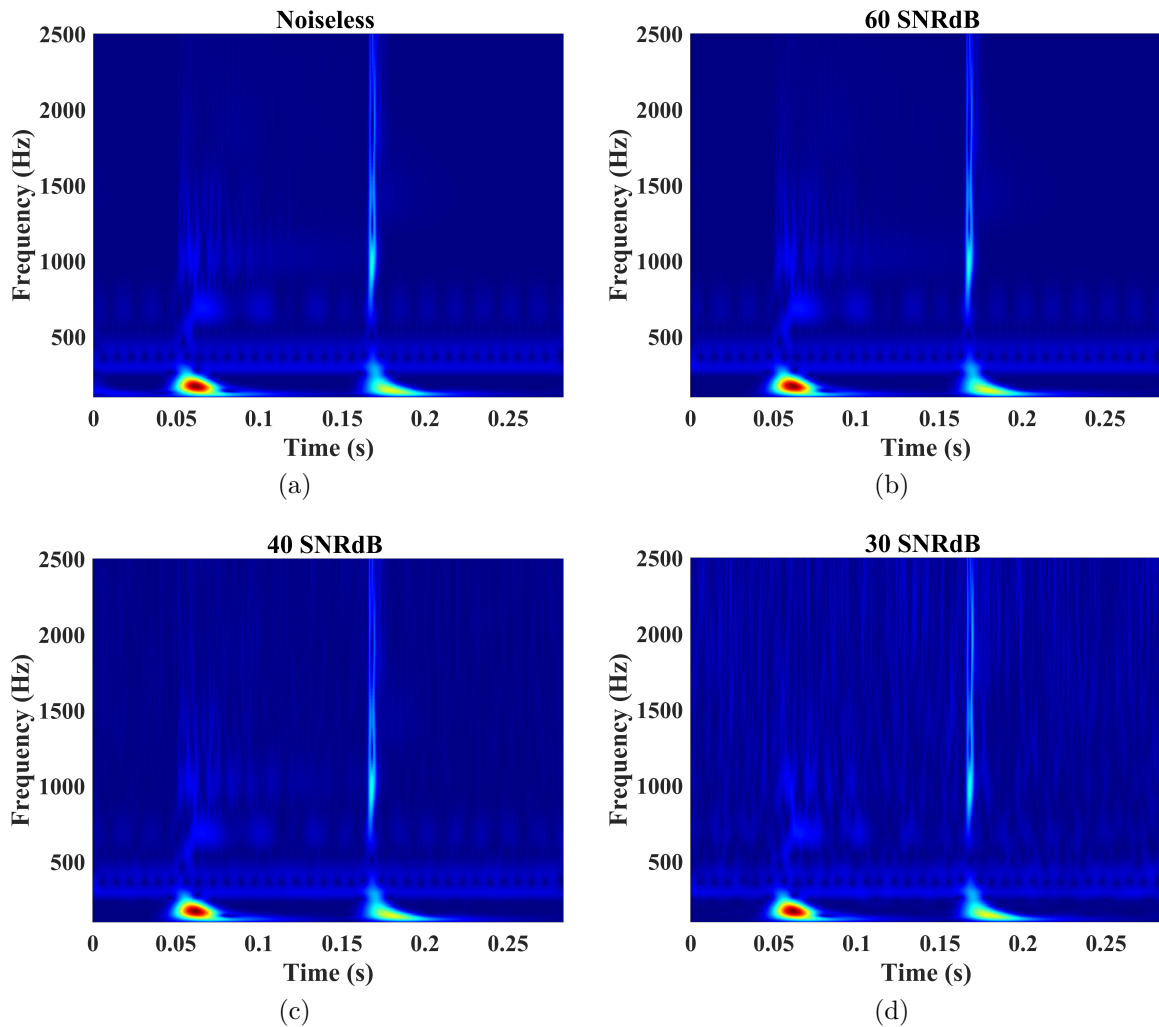
Figure 3.3 – Scalogram Images with Voltage Swell: Noiseless (a), 60 SNRdB (b), 40 SNRdB (c), 30 SNRdB (d).

with a computational effort at the level of precision. More information could be found in (MATHWORKS, 2020c), also the architectures information. Figure 3.4 shows the CNN from scratch layout. The Appendix C contains table details of the layers for each CNN.

After that, the training parameters were defined. Below are some criteria.

- The optimization training method fixed was the SGDM. Other available methods have been tested previously, in the stage of familiarization with the techniques. The choice was based on the speed of training and the simplicity that the method updates the weights.

- The final learning rate α for CNN elaborated by the author was 0.01, after attempts at 0.0001, 0.001 and 0.1. For pre-trained networks, the choice was based on the slow learning characteristics of these networks. Thus, $\alpha = 0.0001$ was attributed to these since higher values caused optimization gradient stagnation in a minimum location, and the accuracy was below 50%.
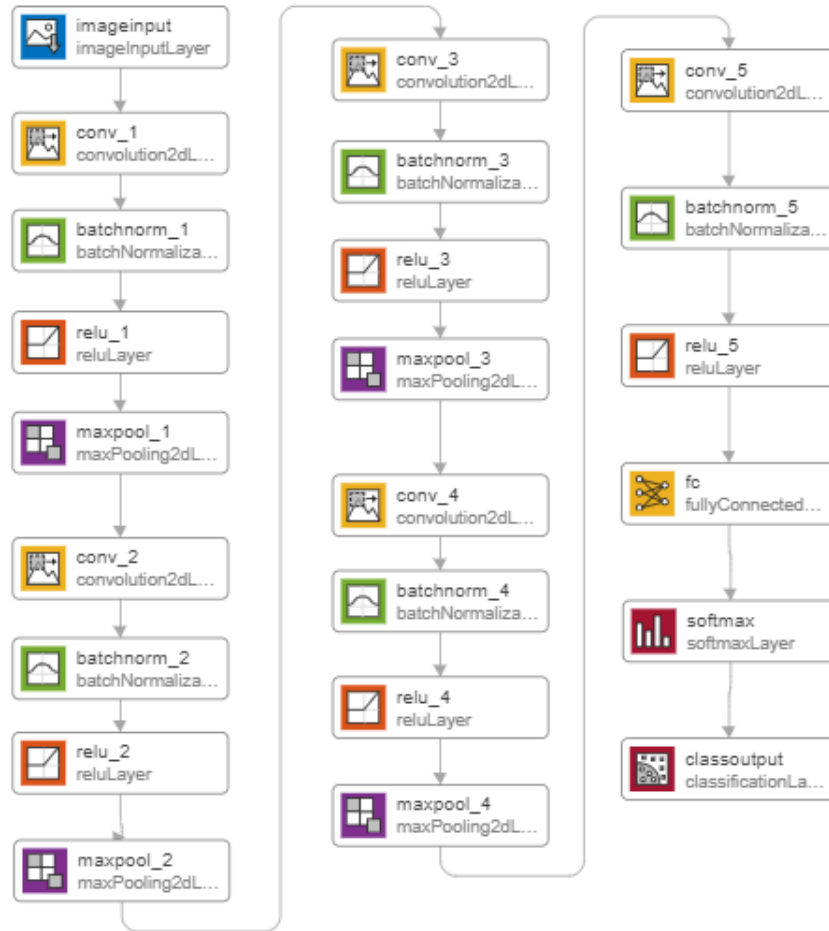
Figure 3.4 – CNN from scratch architecture.

- Regarding accuracy, in the training stage the objective was 100% in this stage.

From the image dataset for training, 80% (3840) were separated for training and 20% (960) for validation. The labels are assigned to each PQ disturbance, with the tag similar to the events' name. Table 3.5 details the training parameters.

Table 3.5 – CNNs Training Parametrs and Features

Parameters	CNN from Scratch	SqueezeNet	GoogleNet	ResNet-50
Optimization	SGDM	SGDM	SGDM	SGDM
Learning Rate	0.01	0.0001	0.0001	0.0001
Max Epoch	4	4	4	4
Mini-Batch Size	24	24	24	24
Number of Layers	23	68	144	177
Input Size	240x240x3	227x227x3	224x224x3	224x224x3

It is necessary to highlight that the objective of this final evaluation of the work is not to determine better values to be used in models, but how the models can be applied with many times high accuracy and simplicity of implementation. The figure 3.5 shows the performances of each network.
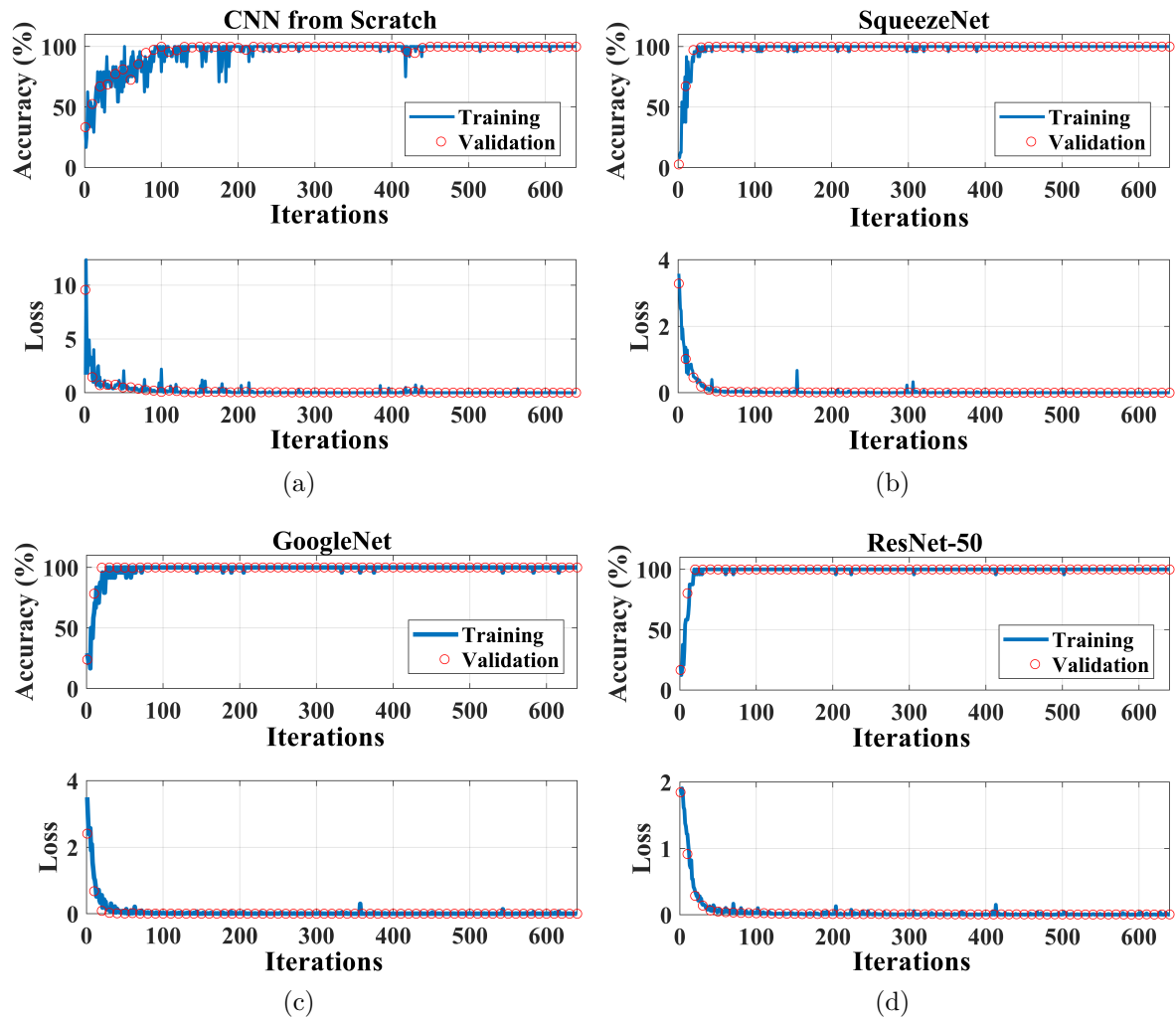
Figure 3.5 – Deep Networks Training: CNN from Scratch (a), SqueezeNet (b), GoogleNet (c), and ResNet-50 (d).

It is observed that all of them obtained good results in this training stage, with a final accuracy of 100%, which remained for most of the training as well, departing almost nothing from the validation. Thus, it is possible to state that the networks presented here in this work present a good performance in training. The duration of each training highlights the computational effort to train each network. As for the duration of each training, below:

- **CNN from Scratch:** 87 minutes;

- **SqueezeNet:** 66 minutes;

- **GoogleNet:** 111 minutes;

- **ResNet-50:** 273 minutes.

The computer used for the training and classification stage is a LENOVO IDEA-PAD 320, with an Intel (R) Core (TM) i5-8250OU CPU @ 1.60GHz 1.80 GHz, 8 GB of RAM, and a 64-bit Windows operating system.

4 Results and Discussion

In this chapter, the results are presented with each proposed CNN classification results for the tests set. In this way, it is possible to verify the models' validity and compare the classification performance through accuracy. A discussion of the results found and outputs of the methodology is also taken into consideration.

4.1 Performances and Results

In this step, the test set generated in bar 4 of the 230 kV system models was used, with 300 signals (50 of each class). In this way, the networks classified this set to four noise levels with SNR= 30, 40 and 60 dB. The confusion matrix and the total and specific accuracy values of each class were used to illustrate the results. The confusion matrix allows a numerical visualization between predicted classes and real classes of the test set. It also indicates the quantity correctly classified, quantity incorrectly typed, and what confusions were made between the classes. The code used to generate the classification results and the confusion matrices are found in Appendix B.

The CNN from Scratch showed high accuracy in the test set, with a total accuracy of 97.67% for signals without noise, 97.33% for signals with 40 and 60 SNRdB, and 96.67% for signals 30 SNRdB. Figure 4.1 illustrates the confusion matrices obtained for CNN from Scratch. It is already possible to begin to notice some confusions are the result of wrong classifications of events that involve short-term variation of RMS. Table 4.1 shows the accuracy for each class for this results.

Table 4.1 – CNN from Scratch accuracy for each class.

Class	Noiseless	60 SNRdB	40 SNRdB	30 SNRdB
Normal	100%	100%	100%	100%
Impulsive	100%	100%	100%	100%
Interruption	100%	100%	100%	100%
Oscillatory	100%	98%	98%	98%
Sag	100%	100%	100%	100%
Swell	86%	86%	86%	82%

SqueezeNet does not present an exciting result in this stage, with a total accuracy of 72.33% for signals without noise and 40 SNRdB, 72% for signals with 60 SNRdB, and 66.67% for signals with 30 SNRdB. This result reflects a lot the low accuracy characteristic of this pre-trained network. In the classification performance, this network has often qualified transient impulsive events and voltage sag as swells, for sags is almost all wrong.
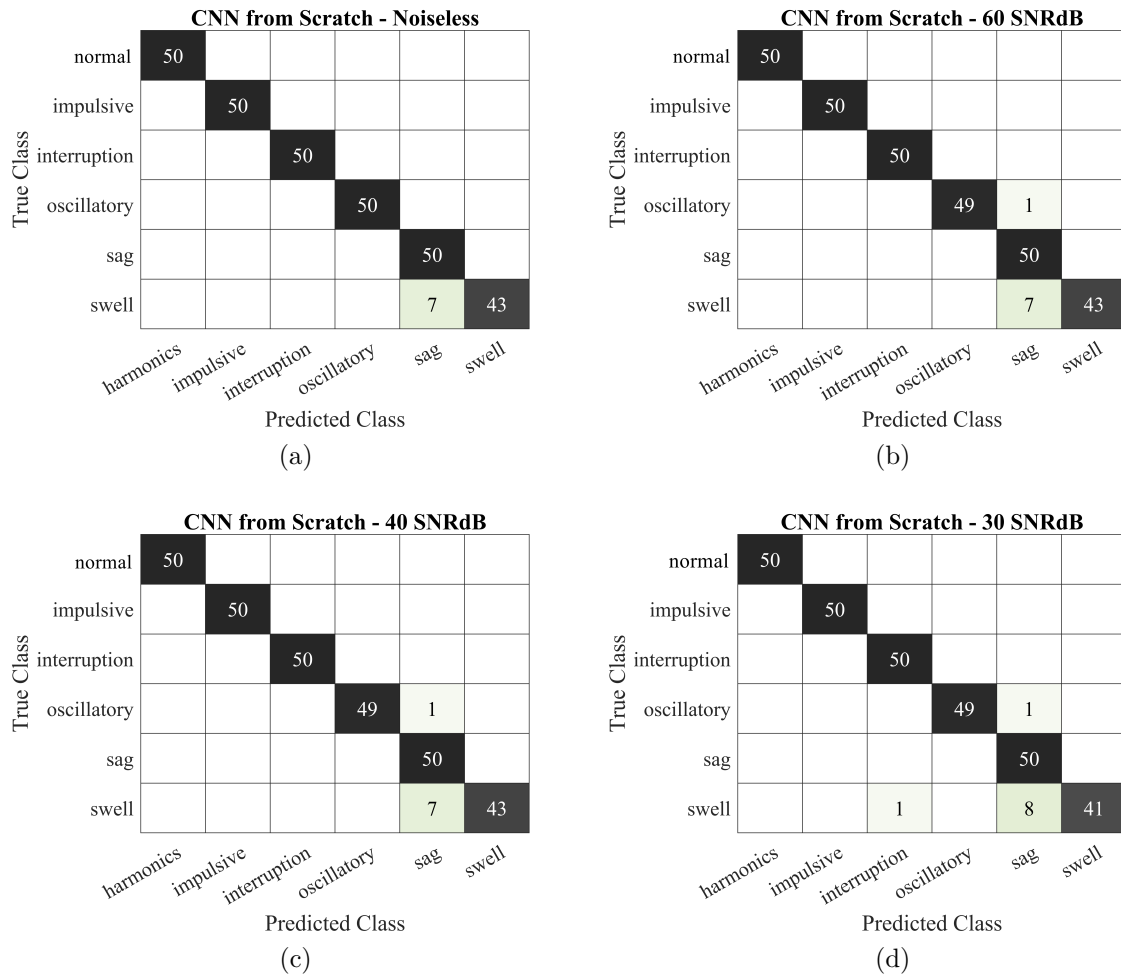
Figure 4.1 – CNN from Scratch Test Results: Noiseless (a), 60 SNRdB (b), 40 SNRdB (c), and 30 SNRdB (d).

Figure 4.2 shows the confusion matrices for SqueezeNet. Table 4.2 details the accuracy of each class.

Table 4.2 – CNN SqueezeNet accuracy for each class.

Class	Noiseless	60 SNRdB	40 SNRdB	30 SNRdB
Normal	100%	100%	100%	100%
Impulsive	34%	34%	34%	2%
Interruption	100%	100%	100%	100%
Oscillatory	100%	98%	98%	98%
Sag	0%	0%	2%	0%
Swell	100%	100%	100%	100%

GoogleNet is a network with relatively low accuracy. It was also reflected in the results. This CNN showed a total accuracy of 80% for noiseless signals and signals with 60 SNRdB. For signals with 40 SNRdB, it obtained 77.67% and 70.67% for 30 SNRdB. The network started to err significantly with transient impulsive signals as the noise increased, presenting a low accuracy for this class and voltage sag. Figure 4.3 shows the confusions
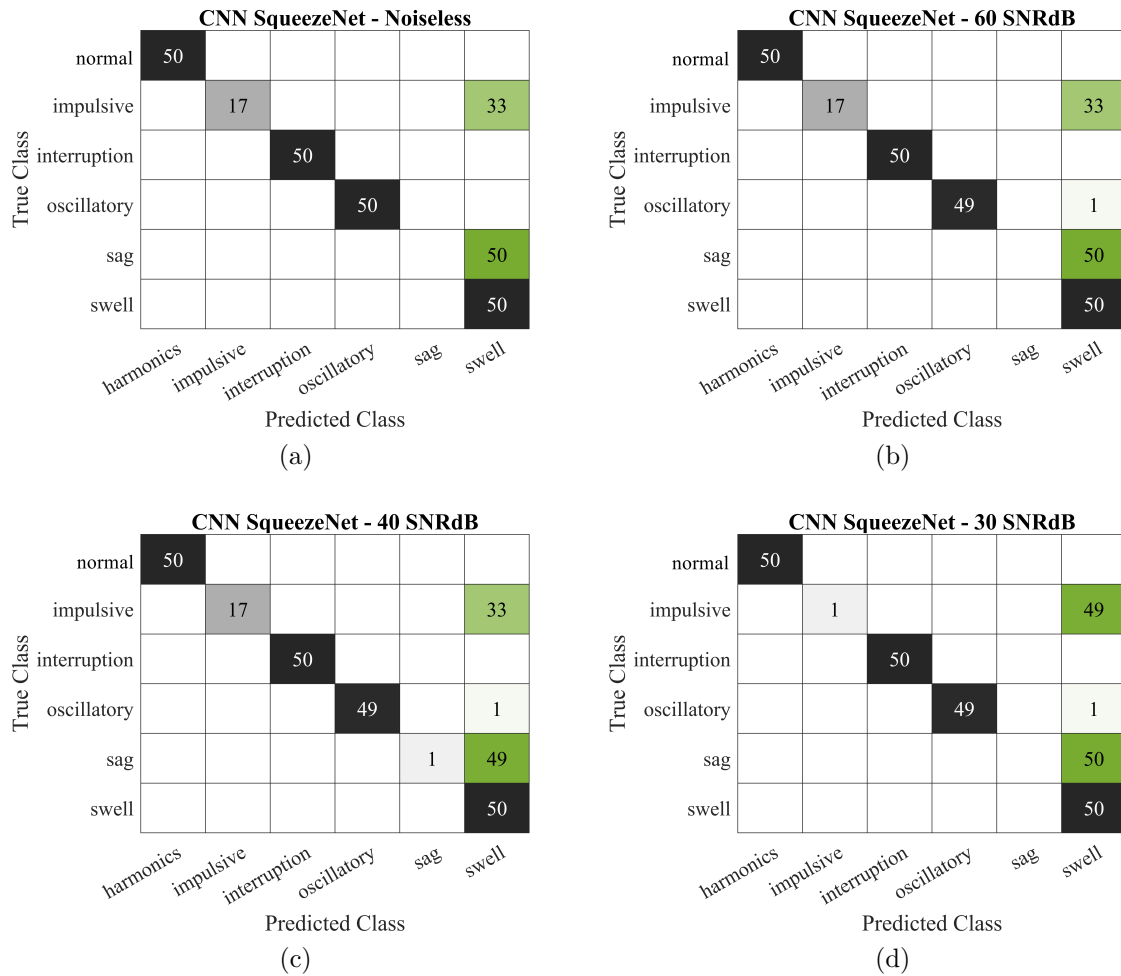
Figure 4.2 – SqueezeNet Scratch Test Results: Noiseless (a), 60 SNRdB (b), 40 SNRdB (c), and 30 SNRdB (d).

matrices for GoogleNet classification. Table 4.3 details the GoogleNet accuracy of each class.

Table 4.3 – CNN GoogleNet accuracy for each class.

Class	Noiseless	60 SNRdB	40 SNRdB	30 SNRdB
Normal	100%	100%	100%	100%
Impulsive	64%	64%	52%	0%
Interruption	100%	100%	100%	100%
Oscillatory	100%	100%	100%	100%
Sag	16%	16%	14%	24%
Swell	100%	100%	100%	82%

Finally, ResNet-50 achieved the best performance among CNNs. It has achieved total accuracy greater than CNN from Scratch. The total accuracy obtained is 100% for noiseless, 60 SNRdB and 40 SNRdB. With only 5 classification errors of the sag class for swell, it obtained 98.3% for signals with 30 SNRdB. Figure 4.4 shows the ResNet-50 confusion matrices. Table 4.4 details the ResNet-50 accuracy for each class.
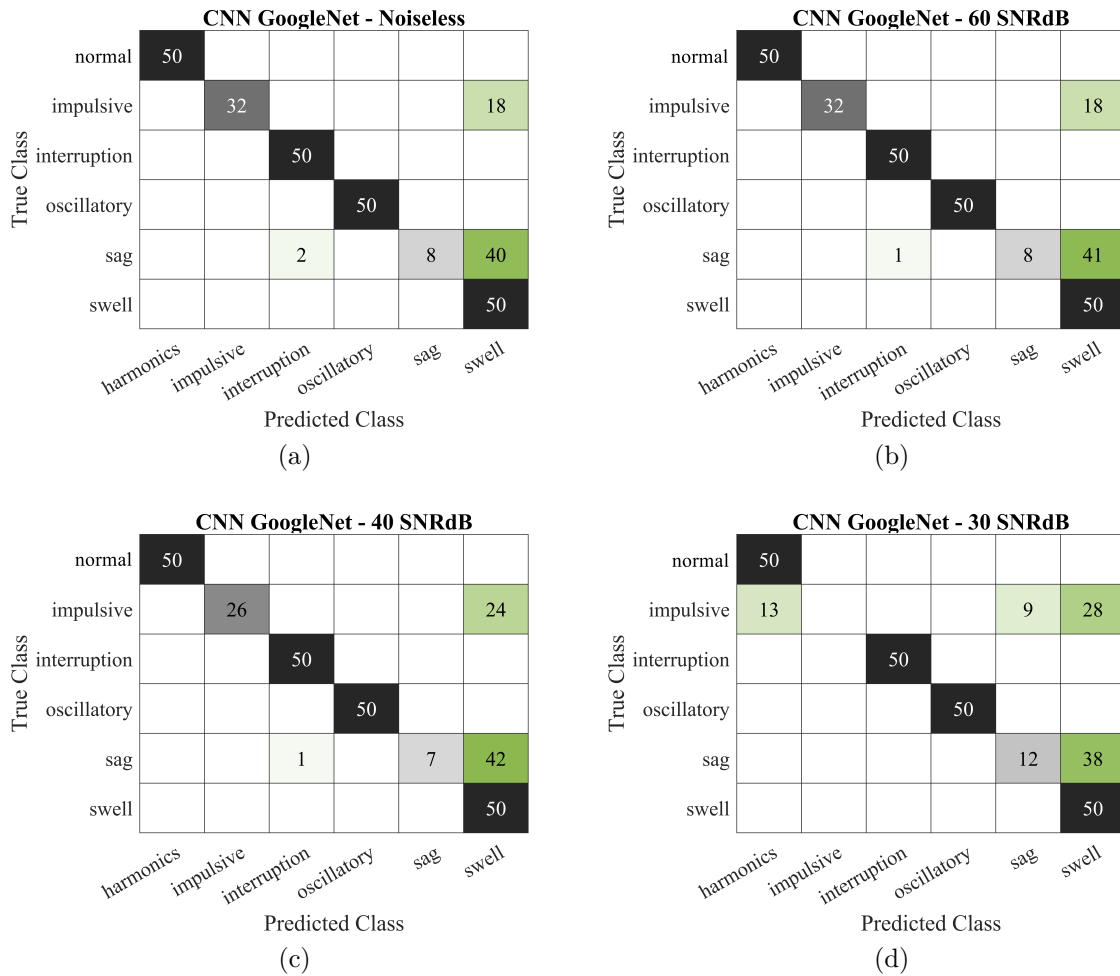
Figure 4.3 – GoogleNet Test Results: Noiseless (a), 60 SNRdB (b), 40 SNRdB (c), and 30 SNRdB (d).

Table 4.4 – CNN ResNet-50 accuracy for each class.

Class	Noiseless	60 SNRdB	40 SNRdB	30 SNRdB
Normal	100%	100%	100%	100%
Impulsive	100%	100%	100%	0%
Interruption	100%	100%	100%	100%
Oscillatory	100%	100%	100%	100%
Sag	100%	100%	100%	90%
Swell	100%	100%	100%	100%

For an overview of the results, in most cases, the networks were formidable. The SqueezeNet and GoogleNet networks did not have such good results, showing high accuracy for some classes and others reaching 0%. It causes these networks to lose their total accuracy and do not get the objective of classifying and pattern recognition for all categories. On the other hand, CNN from Scratch and ResNet-50 were the result of state-of-art accuracy. It can be said. Table 4.5 shows a summary of the total accuracy for CNNs produced in this research work.
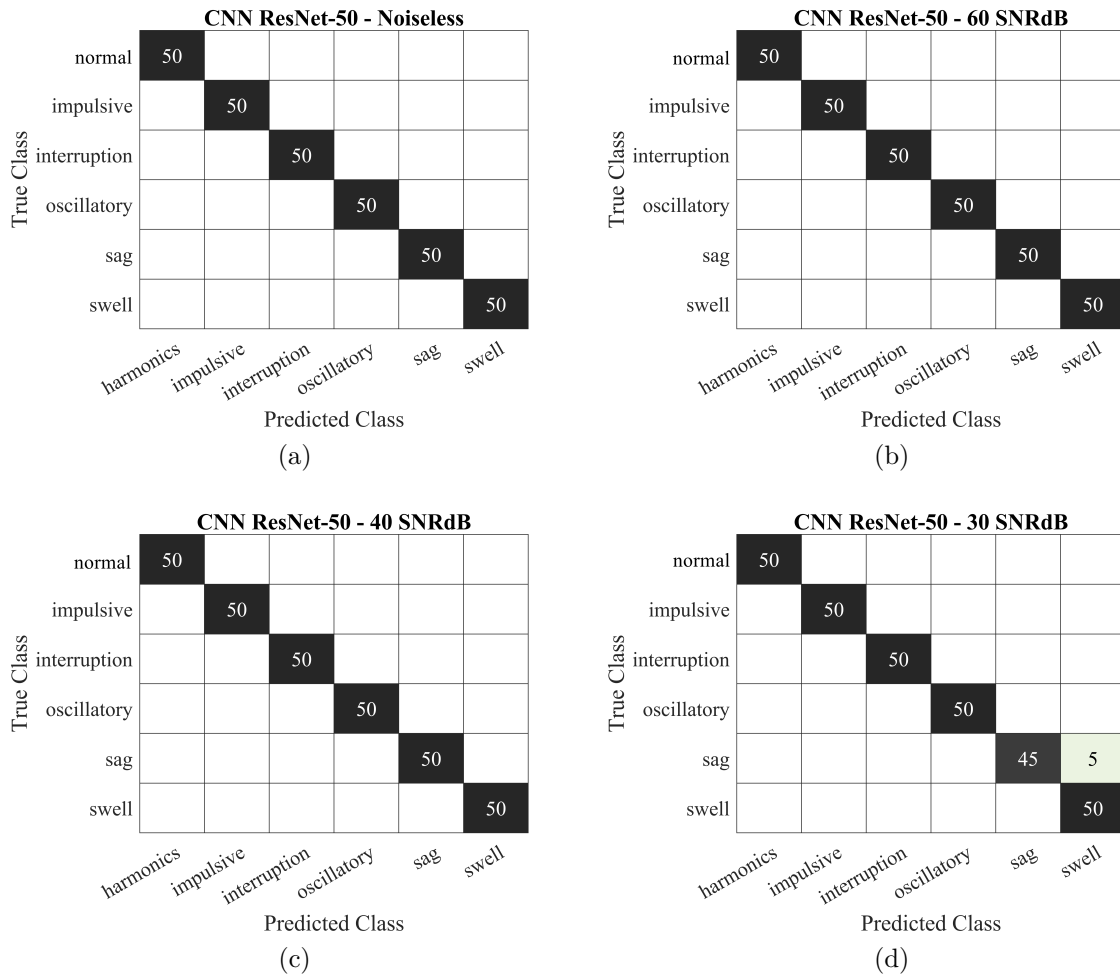
Figure 4.4 – ResNet-50 Test Results: Noiseless (a), 60 SNRdB (b), 40 SNRdB (c), and 30 SNRdB (d).

Table 4.5 – Resume of Total Accuracy for each CNN.

CNN	Noiseless	60 SNRdB	40 SNRdB	30 SNRdB
CNN from Scratch	97.67%	97.33%	97.33%	96.67%
SqueezeNet	72.33%	72%	72.33%	66.67%
GoogleNet	80%	80%	77.67%	70.67%
ResNet-50	100%	100%	100%	98.3%

The best cases obtained in this work are compared with some references' accuracy to highlight the place of the results within state-of-art. The criterion uses references with similar methodologies and accuracy with noiseless signals since each one applies different values in dB. Table 4.6 shows that comparison. When comparing with these other methods, it is possible to verify that satisfactory results were obtained.

Another difference between these and other methodologies is that this work considers only five classes of PQ events. However, the signals are generated from a transmission system model that seeks to approach reality. That is, real signs present harmonics and

Table 4.6 – Comparison with some references.

Method	Accuracy
CWT-CNN from Scratch	97.67%
CWT-ResNet50	100%
WVD-CNN (CAI et al., 2019)	99.67%
TSI-CNN (AHAJJAM et al., 2020)	97.84%
CWT-Bayesyan CNN (EKICI et al., 2020)	99.80%
FFT-CNN (XUE et al., 2020)	99.61%
ResNet-50 (WANG; CHEN, 2019)	99.84%

noise. Many methodologies consider these combinations, but they also use signals without harmonics and are often generated by mathematical functions. In this research, typical signals were developed for training and testing.

4.2   Discussion and Considerations

The results were able to detect this application's potential obtaining results with high accuracy in the classification of PQ disturbances. The exciting thing is that in the pre-trained models, the characteristic accuracy was reflected in the results. And the model made from scratch also obtained an optimal performance. Thus, it is possible to affirm that the objective of creating classification models for pattern recognition in PQ signals using images obtained by signal processing has been achieved. The use of confusion matrix and detailing the class's accuracy brought a positive point to highlight the results since they were enough to directly and concisely describe the performance. These results will be highlighted together with an overview of the work in the next chapter.

5 Conclusions

In this chapter, a retrospective of what was developed and the conclusions about the research are presented. Besides, future work opportunities are highlighted, and a philosophical discussion about the role of key concepts is raised.

5.1 Research Conclusions

This master's dissertartion is a research product that sought to investigate the use of advanced signal processing and DL techniques to classify PQ disturbances. In its first stage, the state-of-art of the use of AI and signal processing for this type of pattern recognition was highlighted and the main theoretical concepts that served as a basis for development. The application's role in the PQ and SG context was also highlighted, making it favorable in a horizon of transformation and increased complexity of the power systems.

This work's main objective was to use CWT with a filter bank to generate scalograms that extrude signal patterns with PQ events through a time-frequency representation, so it was possible to use CNN to classify these 2-D images. MATLAB software was used as the primary tool for all stages: modeling a typical system to generate sets of data for training and classification; use of CWT with filter bank to generate scalograms from a color map, to highlight the characteristics of each signal class; training of CNNs, one from scratch and three from the transfer learning method (SqueezeNet, GoogleNet, and ResNet-50); finally, use the deep layer networks to classify a set of signals for testing.

All stages had their specific objectives completed, culminating in a good execution and development of the research. The results obtained showed high accuracy for CNN from Scratch and ResNet-50, within the highest results (noiseless signals) of each network, they obtained 97.67 % and 100 % accuracy. The other two networks, SqueezeNet and GoogleNet, got good results only for some classes. For others, they did not have the same success in the classification process. The justification for these results was evidenced for transfer learning-based CNN, which has to do with the network's accuracy for the purpose it was designed for. When comparing with other methodologies, with some considerations, the two models with greater accuracy generated in this research are at a high level of performance in the state-of-art.

The use of typical signals, with harmonics and noises, guarantees an approximation with real signals, increasing the results' validity. The work highlighted the role of advanced signal processing in combination with the DL technique forPQ studies in SG. Making codes

and programs available also guarantees a starting point for expanding and exploring the type of application. Along with the detailed description of all stages, it is possible to highlight the research's more excellent reproducibility.

5.2   Future Works

Future work should consider the following opportunities:

- Use more massive datasets with real signs. Despite being a problematic proposal due to the difficulty of having access to a sufficient number of natural and representative data, this would increase the methodology's reliability and applicability.

- Use methodologies such as hardware-in-the-loop / processor-in-the-loop for real-time applications. Besides, greater processing capacity should be sought to expand the research scope since this type of application with images and DL costs a tremendous computational effort.

- It should also consider using the DL technique in conjunction with other ML techniques for classification. In this approach, CNN would play the role of feature extraction to increase accuracy of techniques such as decision tree, support vector machine, multilayer perceptron, etc.

- Finally, using other signal processing techniques for feature extraction and image generation can be considered, such as Stockwell Transform, Curvelet Transform, Hilbert-Huang Transform, Space Phasor Model, among others.

5.3   Philosophical Assessment for Advanced Signal Processing and AI Role in Smart Grids

In this philosophical consideration regarding the role of AI and advanced signal processing technologies, is presented a holistic perspective on the development and design of these technologies in the impact of smart grids. Instead, it is essential to highlight the importance of a normative view of research systems that involve a complex scope, such as smart grids. The future networks that are being developed in the present must address complete solutions that consider all the interactions of the power systems and all interested stakeholders. The emergence of solutions is inherent to normativity and innovation associated with the concept of SG.

To understand the role of advanced signal processing and AI, the author will make an analogy for illustration. See, it is possible to compare the power system to a human body. Both are complex, with critical functioning, dynamic and intelligent. Under this

umbrella are the PQ issues, which we can easily relate to diseases that affect the human body. As well as the symptoms, the PQ disturbances indicate a non-adequacy of the subsystems/bodies within the normality patterns. Thus, advanced signal processing has the same importance as modern medical examinations that discover hidden or confusing diseases from a simple point of view. The advancement of medical tests today allows access to magnetic resonances, tomographies, etc. Also, techniques such as CWT will enable us to bring visualizations in different electrical signals domains. However, a medical examination alone does not have the power to activate actions that allow diagnosing the human being. For that, one must dedicate the specialist knowledge of the medical professional. There comes the role of artificial intelligence, which will emulate the electrical engineer's expert knowledge to classify and efficiently diagnose the different signal processing results.

Therefore, with the increase in criticality and the emergence of new contexts of complexity in the power systems, it is essential for an excellent and reliable operation of SG that innovative solutions emerge, especially in PQ.

Bibliography

AGGARWAL, A. et al. A novel hybrid architecture for classification of power quality disturbances. In: *2019 6th International Conference on Control, Decision and Information Technologies (CoDIT)*. IEEE, 2019. p. 1829–1834. ISBN 978-1-7281-0521-5. Disponível em: <https://ieeexplore.ieee.org/document/8820557/>.

AHAJJAM, M. A. et al. Electric Power Quality Disturbances Classification based on Temporal-Spectral Images and Deep Convolutional Neural Networks. In: *2020 International Wireless Communications and Mobile Computing (IWCMC)*. IEEE, 2020. p. 1701–1706. ISBN 978-1-7281-3129-0. Disponível em: <https://ieeexplore.ieee.org/document/9148438/>.

ALPAYDIN, E. *Machine Learning: The New AI*. MIT Press, 2016. ISBN 0262529513. Disponível em: <https://mitpress.mit.edu/books/machine-learning>.

ALSHAHRANI, S. et al. Evaluation and classification of power quality disturbances based on discrete Wavelet Transform and artificial neural networks. In: *2015 50th International Universities Power Engineering Conference (UPEC)*. [S.l.: s.n.], 2015. p. 1–5. ISBN VO -.

ARRILLAGA, J.; BOLLEN, M. H. J.; WATSON, N. R. Power quality following deregulation. *Proceedings of the IEEE*, v. 88, n. 2, p. 246–261, 2000. ISSN 1558-2256 VO - 88.

BAGHERI, A. *Artificial Intelligence-Based Characterization and Classification Methods for Power Quality Data Analytics*. 213 p. Tese (Doutorado) — Luleå University of Technology, Energy Science, Department of Engineering Sciences and Mathematics, Luleå University of Technology, 2018. Disponível em: <http://ltu.diva-portal.org/smash/get/diva2:1260152/FULLTEXT01.pdfhttp://urn.kb.se/resolve?urn=urn:nbn:se:ltu:diva-71413>.

BALOUJI, E.; SALOR, O. Classification of power quality events using deep learning on event images. In: *2017 3rd International Conference on Pattern Recognition and Image Analysis (IPRIA)*. [S.l.: s.n.], 2017. p. 216–221. ISBN VO -.

BEALE, M. H.; HAGAN, M. T.; DEMUTH, H. B. *Deep Learning Toolbox™ User's Guide*. MathWorks, 2020. Disponível em: <https://www.mathworks.com/help/deeplearning/>.

BHANDAKKAR, A. A.; MATHEW, L. Real-Time-Simulation of IEEE-5-Bus Network on OPAL-RT-OP4510 Simulator. *IOP Conference Series: Materials Science and Engineering*, v. 331, p. 012028, mar 2018. ISSN 1757-8981. Disponível em: <https://iopscience.iop.org/article/10.1088/1757-899X/331/1/012028>.

BHAVANI, R.; PRABHA, N. R. A hybrid classifier for power quality (PQ) problems using wavelets packet transform (WPT) and artificial neural networks (ANN). In: *2017 IEEE International Conference on Intelligent Techniques in Control, Optimization and Signal Processing (INCOS)*. [S.l.: s.n.], 2017. p. 1–7. ISBN VO -.

BOLLEN, M.; STYVAKTAKIS, E.; GU, I. Categorization and Analysis of Power System Transients. *IEEE Transactions on Power Delivery*, v. 20, n. 3, p. 2298–2306, jul 2005. ISSN 0885-8977. Disponível em: <http://ieeexplore.ieee.org/document/1458910/>.

BOLLEN, M. H. J.; GU, I. Y.-H. *Signal Processing of Power Quality Disturbances*. Hoboken, NJ, USA: John Wiley & Sons, Inc., 2006. ISBN 9780471931317. Disponível em: <http://doi.wiley.com/10.1002/0471931314>.

BRACALE, A. et al. Guest editorial introduction to the special issue on "advanced signal processing techniques and telecommunications network infrastructures for smart grid analysis, monitoring, and management". *EURASIP Journal on Advances in Signal Processing*, v. 2015, n. 1, p. 48, dec 2015. ISSN 1687-6180. Disponível em: <https://asp-eurasipjournals.springeropen.com/articles/10.1186/s13634-015-0230-1>.

CAI, K. et al. Classification of Power Quality Disturbances Using Wigner-Ville Distribution and Deep Convolutional Neural Networks. *IEEE Access*, v. 7, p. 119099–119109, 2019. ISSN 2169-3536 VO - 7.

CERQUEIRA, A. S. et al. Power quality events recognition using a SVM-based method. *Electric Power Systems Research*, v. 78, n. 9, p. 1546–1552, 2008. ISSN 0378-7796.

CHATTOPADHYAY, S.; MITRA, M.; SENGUPTA, S. *Electric Power Quality*. Dordrecht: Springer Netherlands, 2011. (Power Systems). ISBN 978-94-007-0634-7. Disponível em: <http://link.springer.com/10.1007/978-94-007-0635-4>.

CHEN, C. L. P. Deep learning for pattern learning and recognition. In: *2015 IEEE 10th Jubilee International Symposium on Applied Computational Intelligence and Informatics*. [S.l.: s.n.], 2015. p. 17. ISBN VO -.

COLLINSON, A.; STONES, J. Power quality. *Power Engineering Journal*, v. 15, n. 2, p. 58–64, apr 2001. ISSN 0950-3366. Disponível em: <https://digital-library.theiet.org/content/journals/10.1049/pe{_}20010>.

DONG, Y. et al. A Novel Method for Multiple Power Quality Disturbances Classification Using a Multi-Task Convolution Neural Network. In: *2019 4th International Conference on Power and Renewable Energy (ICPRE)*. [S.l.: s.n.], 2019. p. 274–278. ISBN VO -.

DUGAN, R. C. et al. *Electrical Power Systems Quality, Third Edition*. [S.l.]: McGraw-Hill Professional, 2012. –1 p. ISBN 0071761551.

EKICI, S. et al. Power quality event classification using optimized Bayesian convolutional neural networks. *Electrical Engineering*, jul 2020. ISSN 0948-7921. Disponível em: <http://link.springer.com/10.1007/s00202-020-01066-8>.

GALLI, A. W.; HEYDT, G. T.; RIBEIRO, P. F. Exploring the power of wavelet analysis. *IEEE Computer Applications in Power*, v. 9, n. 4, p. 37–41, 1996. ISSN 1558-4151 VO - 9.

GHAREKHAN, A. H. et al. Distinguishing Cancer and Normal Breast Tissue Autofluorescence Using Continuous Wavelet Transform. *IEEE Journal of Selected Topics in Quantum Electronics*, v. 16, n. 4, p. 893–899, 2010. ISSN 1558-4542 VO - 16.

GONG, R.; RUAN, T. A New Convolutional Network Structure for Power Quality Disturbance Identification and Classification in Micro-Grids. *IEEE Access*, v. 8, p. 88801–88814, 2020. ISSN 2169-3536. Disponível em: <https://ieeexplore.ieee.org/document/9089024/>.

GOU, L. et al. Aeroengine Control System Sensor Fault Diagnosis Based on CWT and CNN. *Mathematical Problems in Engineering*, Hindawi, v. 2020, p. 5357146, 2020. ISSN 1024-123X. Disponível em: <https://doi.org/10.1155/2020/5357146>.

HAMEED, Z.; YOUSAF, A.; Khan Sial, M. Harmonics in Electrical Power Systems and how to remove them by using filters in ETAP. In: *3rd Int. Conf. on Engineering and Emerging Technologies*. [S.l.: s.n.], 2016.

IEEE. *IEEE Recommended Practice for Monitoring Electric Power Quality*. 2019. 1–98 p.

IEEE SA. *IEEE Smart Grid Vision for Computing: 2030 and Beyond*. 2013. 1–133 p.

JAIN, S. Power Quality. In: *Modeling and Control of Power Electronics Converter System for Power Quality Improvements*. Elsevier, 2018. p. 1–29. Disponível em: <https://linkinghub.elsevier.com/retrieve/pii/B9780128145685000016>.

KAZIBWE, W. E. et al. Power quality: a review. *IEEE Computer Applications in Power*, v. 3, n. 1, p. 39–42, 1990. ISSN 1558-4151 VO - 3.

KHAN, S. et al. A Guide to Convolutional Neural Networks for Computer Vision. *Synthesis Lectures on Computer Vision*, v. 8, n. 1, p. 1–207, feb 2018. ISSN 2153-1056. Disponível em: <http://www.morganclaypool.com/doi/10.2200/S00822ED1V01Y201712COV015>.

KHUFFASH, K. A. Smart grids—Overview and background information. In: *Application of Smart Grid Technologies*. Elsevier, 2018. p. 1–10. Disponível em: <https://linkinghub.elsevier.com/retrieve/pii/B9780128031285000015>.

KIM, H. Machine Learning. In: *Design and Optimization for 5G Wireless Communications*. Wiley, 2020. p. 151–193. Disponível em: <https://onlinelibrary.wiley.com/doi/abs/10.1002/9781119494492.ch5>.

KIM, P. *MATLAB Deep Learning*. Berkeley, CA: Apress, 2017. ISBN 978-1-4842-2844-9. Disponível em: <http://link.springer.com/10.1007/978-1-4842-2845-6>.

LI, H. et al. Evaluation of DC Power Quality Based on Empirical Mode Decomposition and One-Dimensional Convolutional Neural Network. *IEEE Access*, v. 8, p. 34339–34349, 2020. ISSN 2169-3536. Disponível em: <https://ieeexplore.ieee.org/document/9000848/>.

LÓPES, L. F. d. M. et al. *Pattern Recognition with Convolutional Neural Networks: Humpback Whale Tails*. [S.l.], 2019. v. 1.

MAHELA, O. P.; SHARMA, U. K.; MANGLANI, T. Recognition of Power Quality Disturbances Using Discrete Wavelet Transform and Fuzzy C-means Clustering. In: *2018 IEEE 8th Power India International Conference (PIICON)*. [S.l.: s.n.], 2018. p. 1–6. ISBN 2642-5289 VO -.

MATHWORKS. *Compute RLC parameters*. 2020. Disponível em: <https://www.mathworks.com/help/physmod/sps/powersys/ref/power_lineparam.html>.

MATHWORKS. *Deep learning approach to train new models faster by using pretrained models.* 2020. Disponível em: <https://www.mathworks.com/discovery/transfer-learning.html>.

MATHWORKS. *Deep Learning for Signal Processing with MATLAB.* 2020. Disponível em: <https://www.mathworks.com/solutions/deep-learning.html>.

MATHWORKS. *Deep Learning Toolbox.* 2020. Disponível em: <https://www.mathworks.com/products/deep-learning.html>.

MATHWORKS. *Options for training deep learning neural network.* 2020. Disponível em: <https://www.mathworks.com/help/deeplearning/ref/trainingoptions.html#bu812m0>.

MATHWORKS. *Pretrained Deep Neural Networks.* 2020. Disponível em: <https://www.mathworks.com/help/deeplearning/ug/pretrained-convolutional-neural-networks.html>.

MATHWORKS. *What Is a Neural Network?* 2020.

MERRY, R. *Wavelet theory and applications: a literature study.* [S.l.]: Technische Universiteit Eindhoven, 2005. (DCT rapporten). DCT 2005.053.

MISHRA, M. et al. Deep learning in electrical utility industry: A comprehensive review of a decade of research. *Engineering Applications of Artificial Intelligence*, v. 96, p. 104000, nov 2020. ISSN 09521976. Disponível em: <https://linkinghub.elsevier.com/retrieve/pii/S0952197620302943>.

MISHRA, P. K.; SUBUDHI, U.; JAIN, S. Power Quality Disturbances Classification with Deep Learning Approach. In: *2019 International Conference on Information Technology (ICIT).* IEEE, 2019. p. 273–278. ISBN 978-1-7281-6052-8. Disponível em: <https://ieeexplore.ieee.org/document/9031954/>.

MORENO-MUÑOZ, A. (Ed.). *Power Quality.* London: Springer London, 2007. (Power Systems). ISBN 978-1-84628-771-8. Disponível em: <http://link.springer.com/10.1007/978-1-84628-772-5>.

MURPHY, K. P. *Machine learning: a probabilistic perspective.* Cambridge, MA: [s.n.], 2012.

NAGATA, E. A. et al. Real-time voltage sag detection and classification for power quality diagnostics. *Measurement*, v. 164, p. 108097, nov 2020. ISSN 02632241. Disponível em: <https://linkinghub.elsevier.com/retrieve/pii/S0263224120306357>.

OZCANLI, A. K.; YAPRAKDAL, F.; BAYSAL, M. Deep learning methods and applications for electrical power systems: A comprehensive review. *International Journal of Energy Research*, v. 44, n. 9, p. 7136–7157, jul 2020. ISSN 0363-907X. Disponível em: <https://onlinelibrary.wiley.com/doi/abs/10.1002/er.5331>.

PERCIVAL, D. B.; WALDEN, A. T. Introduction to Wavelets. In: *Wavelet Methods for Time SeriesAnalysis.* Cambridge: Cambridge University Press, 2000. p. 1–19. Disponível em: <https://www.cambridge.org/core/product/identifier/CBO9780511841040A008/type/book_part>.

QIU, W. et al. An Automatic Identification Framework for Complex Power Quality Disturbances Based on Multifusion Convolutional Neural Network. *IEEE Transactions on Industrial Informatics*, v. 16, n. 5, p. 3233–3241, may 2020. ISSN 1551-3203. Disponível em: <https://ieeexplore.ieee.org/document/8728236/>.

QIU, W. et al. An Automatic Identification Framework for Complex Power Quality Disturbances Based on Multifusion Convolutional Neural Network. *IEEE Transactions on Industrial Informatics*, v. 16, n. 5, p. 3233–3241, 2020. ISSN 1941-0050 VO - 16.

RIBEIRO, P.; POLINDER, H.; VERKERK, M. Planning and Designing Smart Grids: Philosophical Considerations. *IEEE Technology and Society Magazine*, v. 31, n. 3, p. 34–43, 2012. ISSN 0278-0097. Disponível em: <http://ieeexplore.ieee.org/document/6313612/>.

RIBEIRO, P. F. et al. (Ed.). *Power Systems Signal Processing For Smart Grids*. Chichester, United Kingdom: John Wiley and Sons Ltd, 2013. ISBN 9781118639283. Disponível em: <http://doi.wiley.com/10.1002/9781118639283>.

RIOUL, O.; VETTERLI, M. Wavelets and signal processing. *IEEE Signal Processing Magazine*, v. 8, n. 4, p. 14–38, 1991. ISSN 1558-0792 VO - 8.

RÖNNBERG, S.; BOLLEN, M. Power quality issues in the electric power system of the future. *The Electricity Journal*, v. 29, n. 10, p. 49–61, dec 2016. ISSN 10406190. Disponível em: <https://linkinghub.elsevier.com/retrieve/pii/S1040619016302159>.

SHOEB, A.; CLIORD, G. *Chapter 16—Wavelets; Multiscale Activity in Physiological Signals*. 2006.

SHUVO, S. B. et al. A lightweight cnn model for detecting respiratory diseases from lung auscultation sounds using emd-cwt-based hybrid scalogram. *arXiv preprint arXiv:2009.04402*, 2020.

SILVA, L. R. M.; DUQUE, C. A.; RIBEIRO, P. F. Smart signal processing for an evolving electric grid. *EURASIP Journal on Advances in Signal Processing*, v. 2015, n. 1, p. 44, dec 2015. ISSN 1687-6180. Disponível em: <https://asp-eurasipjournals.springeropen.com/articles/10.1186/s13634-015-0229-7>.

SILVA, L. R. M.; DUQUE, C. A.; RIBEIRO, P. F. Power Quality waveform recognition using Google Image Search Engine (iPQ-Google). In: *2016 17th International Conference on Harmonics and Quality of Power (ICHQP)*. [S.l.: s.n.], 2016. p. 1010–1013. ISBN 2164-0610 VO -.

U.S. Department of Energy. *The Smart Grid: An Introduction.* [S.l.], 2008. Disponível em: <https://www.energy.gov/oe/downloads/smart-grid-introduction-0>.

Val Escudero, M. et al. *CIGRE TB 766: JWG C4/B4.38 Network Modelling for Harmonic Studies.* [S.l.: s.n.], 2019.

VIJAYAPRIYA, T.; KOTHARI, D. P. Smart Grid: An Overview. *Smart Grid and Renewable Energy*, v. 02, n. 04, p. 305–311, 2011. ISSN 2151-481X. Disponível em: <http://www.scirp.org/journal/doi.aspx?DOI=10.4236/sgre.2011.24035>.

WANG, J.; XU, Z.; CHE, Y. Power Quality Disturbance Classification Based on Compressed Sensing and Deep Convolution Neural Networks. *IEEE Access*, v. 7, p. 78336–78346, 2019. ISSN 2169-3536. Disponível em: <https://ieeexplore.ieee.org/document/8735661/>.

WANG, S.; CHEN, H. A novel deep learning method for the classification of power quality disturbances using deep convolutional neural network. *Applied Energy*, v. 235, p. 1126–1140, feb 2019. ISSN 03062619. Disponível em: <https://linkinghub.elsevier.com/retrieve/pii/S0306261918314703>.

WANG, X. *Deep Learning in Object Recognition, Detection, and Segmentation*. now, 2016. 1 p. ISBN 9781680831177. Disponível em: <http://ieeexplore.ieee.org/document/8187348>.

WIECHOWSKI, W. T. *Harmonics in transmission power systems* . Aalborg: Institut for Energiteknik, Aalborg Universitet, 2006.

XIN, H. et al. Fracture acoustic emission signals identification of stay cables in bridge engineering application using deep transfer learning and wavelet analysis. *Advances in Bridge Engineering*, v. 1, dec 2020.

XUE, H. et al. A Novel Deep Convolution Neural Network and Spectrogram Based Microgrid Power Quality Disturbances Classification Method. In: *2020 IEEE Applied Power Electronics Conference and Exposition (APEC)*. IEEE, 2020. p. 2303–2307. ISBN 978-1-7281-4829-8. Disponível em: <https://ieeexplore.ieee.org/document/9124252/>.

ZAVODA, F. et al. *Power Quality and EMC Issues with Future Electricity Networks*. [S.l.: s.n.], 2018.

Appendix

APPENDIX A – Published Papers

This appendix lists the work associated with the author's master's degree program financed by the Coordination for the Improvement of Higher Education Personnel - Brazil (CAPES) - Financial Code 001.

- R. S. Salles, B. I. L. Fuly, and P. F. Ribeiro, "Smart Grids: An Integrated Perspective," in Internet of Energy for Smart Cities: Machine Learning Models and Techniques, 1st ed., A. Jindal, N. Kumar, and G. S. Aujla, Eds. CRC Press.

- R. S. Salles, G. C. S. Almeida, B. I. L. Fuly, A. C. Z. de Souza, and P. F. Ribeiro, "Fuzzy Logic-Based Controller for BESS and Load Management in a Microgrid Economic Operation," IEEE T&D Latin America Conference, Sep. 2020 (in press).

- R. S. Salles, A. C. Z. de Souza, and P. F. Ribeiro, "Energy Storage for Peak Shaving in a Microgrid in the Context of Brazilian Time-of-Use Rate," Proceedings, vol. 58, no. 1, p. 16, Sep. 2020, doi: 10.3390/WEF-06913.

- R. S. Salles, G. C. S. Almeida, L. R. M. Silva, C. A. Duque and P. F. Ribeiro, "Visualization of Quality Performance Parameters Using Wavelet Scalograms Images ," in XXIII Congresso Brasileiro de Automática, Nov. 2020.

- R. S. Salles, A. C. Zambroni de Souza, and P. F. Ribeiro, "Exploratory Research of Social Aspects for Smart City Development in Itajubá," in 2020 IEEE International Smart Cities Conference (ISC2), Sep. 2020, pp. 1–8, doi: 10.1109/ISC251055.2020.9239032.

- M. N. S. Silva, R. S. Salles, A. Degan, C. A. Duque and P. F. Ribeiro, "Investigation of Harmonic Current Aggregation in the TBE/Eletronorte Transmission System," in XXIII Congresso Brasileiro de Automática, Nov. 2020.

- J. V. B. Andrade, R. S. Salles, M. N. S. Silva, and B. D. Bonatto, "Falling Consumption and Demand for Electricity in South Africa - A Blessing and a Curse," in 2020 IEEE PES/IAS PowerAfrica, Aug. 2020, pp. 1–5, doi: 10.1109/PowerAfrica49420.2020.9219878.

APPENDIX B – MATLAB Codes

All MATLAB codes and the Simulink program, can be found at:

- \<https://github.com/sallesrds/master_thesis_rafael-s-salles.git\>

APPENDIX C – Trained CNN layers details

In this appendix are the tables with details of the layers of the trained CNNs.

C.1 CNN from Scratch

Table C.1 shows the layers details of CNN from Scratch.

Table C.1 – CNN from Scratch Layers.

N°	Type	Description
1	Image Input	240x240x3 images with 'zerocenter' normalization
2	Convolution	32 3x8x3 convolutions with stride [1 1] and padding 'same'
3	Batch Normalization	Batch normalization with 32 channels
4	ReLU	ReLU
5	Max Pooling	2x2 max pooling with stride [2 2] and padding 'same'
6	Convolution	32 3x16x32 convolutions with stride [1 1] and padding 'same'
7	Batch Normalization	Batch normalization with 32 channels
8	ReLU	ReLU
9	Max Pooling	2x2 max pooling with stride [2 2] and padding 'same'
10	Convolution	32 3x32x32 convolutions with stride [1 1] and padding 'same'
11	Batch Normalization	Batch normalization with 32 channels
12	ReLU	ReLU
13	Max Pooling	2x2 max pooling with stride [2 2] and padding 'same'
14	Convolution	32 3x64x32 convolutions with stride [1 1] and padding 'same'
15	Batch Normalization	Batch normalization with 32 channels
16	ReLU	ReLU
17	Max Pooling	2x2 max pooling with stride [2 2] and padding 'same'
18	Convolution	32 3x128x32 convolutions with stride [1 1] and padding 'same'
19	Batch Normalization	Batch normalization with 32 channels
20	ReLU	ReLU
21	Fully Connected	6 fully connected layer
22	Softmax	softmax
23	Classification Output	crossentropyex with 'harmonics' and 5 other classes

C.2   SqueezeNet

Table C.2 shows the layers details of SqueezeNet.

Table C.2 – SqueezeNet Layers.

N°	Type	Description
1	Image Input	227x227x3 images with 'zerocenter' normalization
2	Convolution	64 3x3x3 convolutions with stride [2 2] and padding [0 0 0 0]
3	ReLU	ReLU
4	Max Pooling	3x3 max pooling with stride [2 2] and padding [0 0 0 0]
5	Convolution	16 1x1x64 convolutions with stride [1 1] and padding [0 0 0 0]
6	ReLU	ReLU
7	Convolution	64 3x3x16 convolutions with stride [1 1] and padding [1 1 1 1]
8	ReLU	ReLU
9	Convolution	64 1x1x16 convolutions with stride [1 1] and padding [0 0 0 0]
10	ReLU	ReLU
11	Depth concatenation	Depth concatenation of 2 inputs
12	Convolution	16 1x1x128 convolutions with stride [1 1] and padding [0 0 0 0]
13	ReLU	ReLU
14	Convolution	64 3x3x16 convolutions with stride [1 1] and padding [1 1 1 1]
15	ReLU	ReLU
16	Convolution	64 1x1x16 convolutions with stride [1 1] and padding [0 0 0 0]
17	ReLU	ReLU
18	Depth concatenation	Depth concatenation of 2 inputs
19	Max Pooling	3x3 max pooling with stride [2 2] and padding [0 1 0 1]
20	Convolution	32 1x1x128 convolutions with stride [1 1] and padding [0 0 0 0]
21	ReLU	ReLU

22	Convolution	128 1x1x32 convolutions with stride [1 1] and padding [0 0 0 0]
23	ReLU	ReLU
24	Convolution	128 3x3x32 convolutions with stride [1 1] and padding [1 1 1 1]
25	ReLU	ReLU
26	Depth concatenation	Depth concatenation of 2 inputs
27	Convolution	32 1x1x256 convolutions with stride [1 1] and padding [0 0 0 0]
28	ReLU	ReLU
29	Convolution	128 1x1x32 convolutions with stride [1 1] and padding [0 0 0 0]
30	Convolution	128 3x3x32 convolutions with stride [1 1] and padding [1 1 1 1]
31	ReLU	ReLU
32	ReLU	ReLU
33	Depth concatenation	Depth concatenation of 2 inputs
34	Max Pooling	3x3 max pooling with stride [2 2] and padding [0 1 0 1]
35	Convolution	48 1x1x256 convolutions with stride [1 1] and padding [0 0 0 0]
36	ReLU	ReLU
37	Convolution	192 3x3x48 convolutions with stride [1 1] and padding [1 1 1 1]
38	Convolution	192 1x1x48 convolutions with stride [1 1] and padding [0 0 0 0]
39	ReLU	ReLU
40	ReLU	ReLU
41	Depth concatenation	Depth concatenation of 2 inputs
42	Convolution	48 1x1x384 convolutions with stride [1 1] and padding [0 0 0 0]
43	ReLU	ReLU
44	Convolution	192 1x1x48 convolutions with stride [1 1] and padding [0 0 0 0]
45	ReLU	ReLU
46	Convolution	192 3x3x48 convolutions with stride [1 1] and padding [1 1 1 1]
47	ReLU	ReLU

48	Depth concatenation	Depth concatenation of 2 inputs
49	Convolution	64 1x1x384 convolutions with stride [1 1] and padding [0 0 0 0]
50	ReLU	ReLU
51	Convolution	256 3x3x64 convolutions with stride [1 1] and padding [1 1 1 1]
52	ReLU	ReLU
53	Convolution	256 1x1x64 convolutions with stride [1 1] and padding [0 0 0 0]
54	ReLU	ReLU
55	Depth concatenation	Depth concatenation of 2 inputs
56	Convolution	64 1x1x512 convolutions with stride [1 1] and padding [0 0 0 0]
57	ReLU	ReLU
58	Convolution	256 1x1x64 convolutions with stride [1 1] and padding [0 0 0 0]
59	ReLU	ReLU
60	Convolution	256 3x3x64 convolutions with stride [1 1] and padding [1 1 1 1]
61	ReLU	ReLU
62	Depth concatenation	Depth concatenation of 2 inputs
63	Dropout	50% dropout
64	Convolution	6 1x1x512 convolutions with stride [1 1] and padding 'same'
65	ReLU	ReLU
66	Global Average Pooling	Global average pooling
67	Softmax	softmax
68	Classification Output	crossentropyex with 'harmonics' and 5 other classes

C.3   GoogleNet

Table C.3 shows the layers details of GoogleNet.

Table C.3 – GoogleNet Layers.

N°	Type	Description
1	Image Input	224x224x3 images with 'zerocenter' normalization
2	Convolution	64 7x7x3 convolutions with stride [2 2] and padding [3 3 3 3]
3	ReLU	ReLU
4	Max Pooling	3x3 max pooling with stride [2 2] and padding [0 1 0 1]
5	Cross Channel Normalization	cross channel normalization with 5 channels per element
6	Convolution	64 1x1x64 convolutions with stride [1 1] and padding [0 0 0 0]
7	ReLU	ReLU
8	Convolution	192 3x3x64 convolutions with stride [1 1] and padding [1 1 1 1]
9	ReLU	ReLU
10	Cross Channel Normalization	cross channel normalization with 5 channels per element
11	Max Pooling	3x3 max pooling with stride [2 2] and padding [0 1 0 1]
12	Convolution	96 1x1x192 convolutions with stride [1 1] and padding [0 0 0 0]
13	ReLU	ReLU
14	Convolution	128 3x3x96 convolutions with stride [1 1] and padding [1 1 1 1]
15	ReLU	ReLU
16	Convolution	64 1x1x192 convolutions with stride [1 1] and padding [0 0 0 0]
17	ReLU	ReLU
18	Convolution	16 1x1x192 convolutions with stride [1 1] and padding [0 0 0 0]
19	ReLU	ReLU
20	Convolution	32 5x5x16 convolutions with stride [1 1] and padding [2 2 2 2]
21	ReLU	ReLU
22	Max Pooling	3x3 max pooling with stride [1 1] and padding [1 1 1 1]

23	Convolution	32 1x1x192 convolutions with stride [1 1] and padding [0 0 0 0]
24	ReLU	ReLU
25	Depth concatenation	Depth concatenation of 4 inputs
26	Convolution	32 1x1x256 convolutions with stride [1 1] and padding [0 0 0 0]
27	Max Pooling	3x3 max pooling with stride [1 1] and padding [1 1 1 1]
28	ReLU	ReLU
29	Convolution	128 1x1x256 convolutions with stride [1 1] and padding [0 0 0 0]
30	ReLU	ReLU
31	Convolution	64 1x1x256 convolutions with stride [1 1] and padding [0 0 0 0]
32	ReLU	ReLU
33	Convolution	96 5x5x32 convolutions with stride [1 1] and padding [2 2 2 2]
34	Convolution	128 1x1x256 convolutions with stride [1 1] and padding [0 0 0 0]
35	ReLU	ReLU
36	Convolution	192 3x3x128 convolutions with stride [1 1] and padding [1 1 1 1]
37	ReLU	ReLU
38	ReLU	ReLU
39	Depth concatenation	Depth concatenation of 4 inputs
40	Max Pooling	3x3 max pooling with stride [2 2] and padding [0 1 0 1]
41	Max Pooling	3x3 max pooling with stride [1 1] and padding [1 1 1 1]
42	Convolution	192 1x1x480 convolutions with stride [1 1] and padding [0 0 0 0]
43	ReLU	ReLU
44	Convolution	16 1x1x480 convolutions with stride [1 1] and padding [0 0 0 0]
45	Convolution	64 1x1x480 convolutions with stride [1 1] and padding [0 0 0 0]
46	ReLU	ReLU
47	ReLU	ReLU

48	Convolution	48 5x5x16 convolutions with stride [1 1] and padding [2 2 2 2]
49	ReLU	ReLU
50	Convolution	96 1x1x480 convolutions with stride [1 1] and padding [0 0 0 0]
51	ReLU	ReLU
52	Convolution	208 3x3x96 convolutions with stride [1 1] and padding [1 1 1 1]
53	ReLU	ReLU
54	Depth concatenation	Depth concatenation of 4 inputs
55	Convolution	112 1x1x512 convolutions with stride [1 1] and padding [0 0 0 0]
56	ReLU	ReLU
57	Max Pooling	3x3 max pooling with stride [1 1] and padding [1 1 1 1]
58	Convolution	24 1x1x512 convolutions with stride [1 1] and padding [0 0 0 0]
59	Convolution	224 3x3x112 convolutions with stride [1 1] and padding [1 1 1 1]
60	ReLU	ReLU
61	ReLU	ReLU
62	Convolution	64 5x5x24 convolutions with stride [1 1] and padding [2 2 2 2]
63	ReLU	ReLU
64	Convolution	160 1x1x512 convolutions with stride [1 1] and padding [0 0 0 0]
65	Convolution	64 1x1x512 convolutions with stride [1 1] and padding [0 0 0 0]
66	ReLU	ReLU
67	ReLU	ReLU
68	Depth concatenation	Depth concatenation of 4 inputs
69	Convolution	128 1x1x512 convolutions with stride [1 1] and padding [0 0 0 0]
70	ReLU	ReLU
71	Convolution	128 1x1x512 convolutions with stride [1 1] and padding [0 0 0 0]
72	ReLU	ReLU

73	Convolution	24 1x1x512 convolutions with stride [1 1] and padding [0 0 0 0]
74	ReLU	ReLU
75	Convolution	64 5x5x24 convolutions with stride [1 1] and padding [2 2 2 2]
76	Convolution	256 3x3x128 convolutions with stride [1 1] and padding [1 1 1 1]
77	ReLU	ReLU
78	Max Pooling	3x3 max pooling with stride [1 1] and padding [1 1 1 1]
79	Convolution	64 1x1x512 convolutions with stride [1 1] and padding [0 0 0 0]
80	ReLU	ReLU
81	ReLU	ReLU
82	Depth concatenation	Depth concatenation of 4 inputs
83	Convolution	112 1x1x512 convolutions with stride [1 1] and padding [0 0 0 0]
84	Convolution	144 1x1x512 convolutions with stride [1 1] and padding [0 0 0 0]
85	ReLU	ReLU
86	ReLU	ReLU
87	Max Pooling	3x3 max pooling with stride [1 1] and padding [1 1 1 1]
88	Convolution	64 1x1x512 convolutions with stride [1 1] and padding [0 0 0 0]
89	ReLU	ReLU
90	Convolution	288 3x3x144 convolutions with stride [1 1] and padding [1 1 1 1]
91	ReLU	ReLU
92	Convolution	32 1x1x512 convolutions with stride [1 1] and padding [0 0 0 0]
93	ReLU	ReLU
94	Convolution	64 5x5x32 convolutions with stride [1 1] and padding [2 2 2 2]
95	ReLU	ReLU
96	Depth concatenation	Depth concatenation of 4 inputs
97	Convolution	32 1x1x528 convolutions with stride [1 1] and padding [0 0 0 0]

98	ReLU	ReLU
99	Convolution	160 1x1x528 convolutions with stride [1 1] and padding [0 0 0 0]
100	Convolution	256 1x1x528 convolutions with stride [1 1] and padding [0 0 0 0]
101	ReLU	ReLU
102	ReLU	ReLU
103	Max Pooling	3x3 max pooling with stride [1 1] and padding [1 1 1 1]
104	Convolution	128 1x1x528 convolutions with stride [1 1] and padding [0 0 0 0]
105	ReLU	ReLU
106	Convolution	128 5x5x32 convolutions with stride [1 1] and padding [2 2 2 2]
107	ReLU	ReLU
108	Convolution	320 3x3x160 convolutions with stride [1 1] and padding [1 1 1 1]
109	ReLU	ReLU
110	Depth concatenation	Depth concatenation of 4 inputs
111	Max Pooling	3x3 max pooling with stride [2 2] and padding [0 1 0 1]
112	Convolution	160 1x1x832 convolutions with stride [1 1] and padding [0 0 0 0]
113	Convolution	32 1x1x832 convolutions with stride [1 1] and padding [0 0 0 0]
114	ReLU	ReLU
115	Max Pooling	3x3 max pooling with stride [1 1] and padding [1 1 1 1]
116	Convolution	320 3x3x160 convolutions with stride [1 1] and padding [1 1 1 1]
117	ReLU	ReLU
118	Convolution	256 1x1x832 convolutions with stride [1 1] and padding [0 0 0 0]
119	ReLU	ReLU
120	Convolution	128 5x5x32 convolutions with stride [1 1] and padding [2 2 2 2]
121	Convolution	128 1x1x832 convolutions with stride [1 1] and padding [0 0 0 0]

122	ReLU	ReLU
123	ReLU	ReLU
124	ReLU	ReLU
125	Depth concatenation	Depth concatenation of 4 inputs
126	Convolution	192 1x1x832 convolutions with stride [1 1] and padding [0 0 0 0]
127	ReLU	ReLU
128	Convolution	384 3x3x192 convolutions with stride [1 1] and padding [1 1 1 1]
129	Convolution	384 1x1x832 convolutions with stride [1 1] and padding [0 0 0 0]
130	ReLU	ReLU
131	Max Pooling	3x3 max pooling with stride [1 1] and padding [1 1 1 1]
132	Convolution	128 1x1x832 convolutions with stride [1 1] and padding [0 0 0 0]
133	ReLU	ReLU
134	ReLU	ReLU
135	Convolution	48 1x1x832 convolutions with stride [1 1] and padding [0 0 0 0]
136	ReLU	ReLU
137	Convolution	128 5x5x48 convolutions with stride [1 1] and padding [2 2 2 2]
138	ReLU	ReLU
139	Depth concatenation	Depth concatenation of 4 inputs
140	Global Average Pooling	Global average pooling
141	Dropout	40% dropout
142	Fully Connected	6 fully connected layer
143	Softmax	softmax
144	Classification Output	crossentropyex with 'harmonics' and 5 other classes

C.4   ResNet-50

Table C.4 shows the layers details of ResNet-50.

Table C.4 – ResNet-50 Layers.

N°	Type	Description
1	Image Input	224x224x3 images with 'zerocenter' normalization
2	Convolution	64 7x7x3 convolutions with stride [2 2] and padding [3 3 3 3]
3	Batch Normalization	Batch normalization with 64 channels
4	ReLU	ReLU
5	Max Pooling	3x3 max pooling with stride [2 2] and padding [1 1 1 1]
6	Convolution	64 1x1x64 convolutions with stride [1 1] and padding [0 0 0 0]
7	Convolution	256 1x1x64 convolutions with stride [1 1] and padding [0 0 0 0]
8	Batch Normalization	Batch normalization with 256 channels
9	Batch Normalization	Batch normalization with 64 channels
10	ReLU	ReLU
11	Convolution	64 3x3x64 convolutions with stride [1 1] and padding 'same'
12	Batch Normalization	Batch normalization with 64 channels
13	ReLU	ReLU
14	Convolution	256 1x1x64 convolutions with stride [1 1] and padding [0 0 0 0]
15	Batch Normalization	Batch normalization with 256 channels
16	Addition	Element-wise addition of 2 inputs
17	ReLU	ReLU
18	Convolution	64 1x1x256 convolutions with stride [1 1] and padding [0 0 0 0]
19	Batch Normalization	Batch normalization with 64 channels
20	ReLU	ReLU
21	Convolution	64 3x3x64 convolutions with stride [1 1] and padding 'same'
22	Batch Normalization	Batch normalization with 64 channels
23	ReLU	ReLU
24	Convolution	256 1x1x64 convolutions with stride [1 1] and padding [0 0 0 0]
25	Batch Normalization	Batch normalization with 256 channels
26	Addition	Element-wise addition of 2 inputs

27	ReLU	ReLU
28	Convolution	64 1x1x256 convolutions with stride [1 1] and padding [0 0 0 0]
29	Batch Normalization	Batch normalization with 64 channels
30	ReLU	ReLU
31	Convolution	64 3x3x64 convolutions with stride [1 1] and padding 'same'
32	Batch Normalization	Batch normalization with 64 channels
33	ReLU	ReLU
34	Convolution	256 1x1x64 convolutions with stride [1 1] and padding [0 0 0 0]
35	Batch Normalization	Batch normalization with 256 channels
36	Addition	Element-wise addition of 2 inputs
37	ReLU	ReLU
38	Convolution	512 1x1x256 convolutions with stride [2 2] and padding [0 0 0 0]
39	Batch Normalization	Batch normalization with 512 channels
40	Convolution	128 1x1x256 convolutions with stride [2 2] and padding [0 0 0 0]
41	Batch Normalization	Batch normalization with 128 channels
42	ReLU	ReLU
43	Convolution	128 3x3x128 convolutions with stride [1 1] and padding 'same'
44	Batch Normalization	Batch normalization with 128 channels
45	ReLU	ReLU
46	Convolution	512 1x1x128 convolutions with stride [1 1] and padding [0 0 0 0]
47	Batch Normalization	Batch normalization with 512 channels
48	Addition	Element-wise addition of 2 inputs
49	ReLU	ReLU
50	Convolution	128 1x1x512 convolutions with stride [1 1] and padding [0 0 0 0]
51	Batch Normalization	Batch normalization with 128 channels
52	ReLU	ReLU
53	Convolution	128 3x3x128 convolutions with stride [1 1] and padding 'same'
54	Batch Normalization	Batch normalization with 128 channels
55	ReLU	ReLU

56	Convolution	512 1x1x128 convolutions with stride [1 1] and padding [0 0 0 0]
57	Batch Normalization	Batch normalization with 512 channels
58	Addition	Element-wise addition of 2 inputs
59	ReLU	ReLU
60	Convolution	128 1x1x512 convolutions with stride [1 1] and padding [0 0 0 0]
61	Batch Normalization	Batch normalization with 128 channels
62	ReLU	ReLU
63	Convolution	128 3x3x128 convolutions with stride [1 1] and padding 'same'
64	Batch Normalization	Batch normalization with 128 channels
65	ReLU	ReLU
66	Convolution	512 1x1x128 convolutions with stride [1 1] and padding [0 0 0 0]
67	Batch Normalization	Batch normalization with 512 channels
68	Addition	Element-wise addition of 2 inputs
69	ReLU	ReLU
70	Convolution	128 1x1x512 convolutions with stride [1 1] and padding [0 0 0 0]
71	Batch Normalization	Batch normalization with 128 channels
72	ReLU	ReLU
73	Convolution	128 3x3x128 convolutions with stride [1 1] and padding 'same'
74	Batch Normalization	Batch normalization with 128 channels
75	ReLU	ReLU
76	Convolution	512 1x1x128 convolutions with stride [1 1] and padding [0 0 0 0]
77	Batch Normalization	Batch normalization with 512 channels
78	Addition	Element-wise addition of 2 inputs
79	ReLU	ReLU
80	Convolution	1024 1x1x512 convolutions with stride [2 2] and padding [0 0 0 0]
81	Batch Normalization	Batch normalization with 1024 channels
82	Convolution	256 1x1x512 convolutions with stride [2 2] and padding [0 0 0 0]
83	Batch Normalization	Batch normalization with 256 channels
84	ReLU	ReLU

85	Convolution	256 3x3x256 convolutions with stride [1 1] and padding 'same'
86	Batch Normalization	Batch normalization with 256 channels
87	ReLU	ReLU
88	Convolution	1024 1x1x256 convolutions with stride [1 1] and padding [0 0 0 0]
89	Batch Normalization	Batch normalization with 1024 channels
90	Addition	Element-wise addition of 2 inputs
91	ReLU	ReLU
92	Convolution	256 1x1x1024 convolutions with stride [1 1] and padding [0 0 0 0]
93	Batch Normalization	Batch normalization with 256 channels
94	ReLU	ReLU
95	Convolution	256 3x3x256 convolutions with stride [1 1] and padding 'same'
96	Batch Normalization	Batch normalization with 256 channels
97	ReLU	ReLU
98	Convolution	1024 1x1x256 convolutions with stride [1 1] and padding [0 0 0 0]
99	Batch Normalization	Batch normalization with 1024 channels
100	Addition	Element-wise addition of 2 inputs
101	ReLU	ReLU
102	Convolution	256 1x1x1024 convolutions with stride [1 1] and padding [0 0 0 0]
103	Batch Normalization	Batch normalization with 256 channels
104	ReLU	ReLU
105	Convolution	256 3x3x256 convolutions with stride [1 1] and padding 'same'
106	Batch Normalization	Batch normalization with 256 channels
107	ReLU	ReLU
108	Convolution	1024 1x1x256 convolutions with stride [1 1] and padding [0 0 0 0]
109	Batch Normalization	Batch normalization with 1024 channels
110	Addition	Element-wise addition of 2 inputs
111	ReLU	ReLU
112	Convolution	256 1x1x1024 convolutions with stride [1 1] and padding [0 0 0 0]
113	Batch Normalization	Batch normalization with 256 channels

114	ReLU	ReLU
115	Convolution	256 3x3x256 convolutions with stride [1 1] and padding 'same'
116	Batch Normalization	Batch normalization with 256 channels
117	ReLU	ReLU
118	Convolution	1024 1x1x256 convolutions with stride [1 1] and padding [0 0 0 0]
119	Batch Normalization	Batch normalization with 1024 channels
120	Addition	Element-wise addition of 2 inputs
121	ReLU	ReLU
122	Convolution	256 1x1x1024 convolutions with stride [1 1] and padding [0 0 0 0]
123	Batch Normalization	Batch normalization with 256 channels
124	ReLU	ReLU
125	Convolution	256 3x3x256 convolutions with stride [1 1] and padding 'same'
126	Batch Normalization	Batch normalization with 256 channels
127	ReLU	ReLU
128	Convolution	1024 1x1x256 convolutions with stride [1 1] and padding [0 0 0 0]
129	Batch Normalization	Batch normalization with 1024 channels
130	Addition	Element-wise addition of 2 inputs
131	ReLU	ReLU
132	Convolution	256 1x1x1024 convolutions with stride [1 1] and padding [0 0 0 0]
133	Batch Normalization	Batch normalization with 256 channels
134	ReLU	ReLU
135	Convolution	256 3x3x256 convolutions with stride [1 1] and padding 'same'
136	Batch Normalization	Batch normalization with 256 channels
137	ReLU	ReLU
138	Convolution	1024 1x1x256 convolutions with stride [1 1] and padding [0 0 0 0]
139	Batch Normalization	Batch normalization with 1024 channels
140	Addition	Element-wise addition of 2 inputs
141	ReLU	ReLU
142	Convolution	2048 1x1x1024 convolutions with stride [2 2] and padding [0 0 0 0]

143	Batch Normalization	Batch normalization with 2048 channels
144	Convolution	512 1x1x1024 convolutions with stride [2 2] and padding [0 0 0 0]
145	Batch Normalization	Batch normalization with 512 channels
146	ReLU	ReLU
147	Convolution	512 3x3x512 convolutions with stride [1 1] and padding 'same'
148	Batch Normalization	Batch normalization with 512 channels
149	ReLU	ReLU
150	Convolution	2048 1x1x512 convolutions with stride [1 1] and padding [0 0 0 0]
151	Batch Normalization	Batch normalization with 2048 channels
152	Addition	Element-wise addition of 2 inputs
153	ReLU	ReLU
154	Convolution	512 1x1x2048 convolutions with stride [1 1] and padding [0 0 0 0]
155	Batch Normalization	Batch normalization with 512 channels
156	ReLU	ReLU
157	Convolution	512 3x3x512 convolutions with stride [1 1] and padding 'same'
158	Batch Normalization	Batch normalization with 512 channels
159	ReLU	ReLU
160	Convolution	2048 1x1x512 convolutions with stride [1 1] and padding [0 0 0 0]
161	Batch Normalization	Batch normalization with 2048 channels
162	Addition	Element-wise addition of 2 inputs
163	ReLU	ReLU
164	Convolution	512 1x1x2048 convolutions with stride [1 1] and padding [0 0 0 0]
165	Batch Normalization	Batch normalization with 512 channels
166	ReLU	ReLU
167	Convolution	512 3x3x512 convolutions with stride [1 1] and padding 'same'
168	Batch Normalization	Batch normalization with 512 channels
169	ReLU	ReLU
170	Convolution	2048 1x1x512 convolutions with stride [1 1] and padding [0 0 0 0]
171	Batch Normalization	Batch normalization with 2048 channels

172	Addition	Element-wise addition of 2 inputs
173	ReLU	ReLU
174	Global Average Pooling	Global average pooling
175	Fully Connected	6 fully connected layer
176	Softmax	softmax
177	Classification Output	crossentropyex with 'harmonics' and 5 other classes